学　位　論　文

PTEN loss is a possible mechanism of trastuzumab resistance in extramammary Paget disease

（PTEN 欠失は乳房外 Paget 病においてトラスツズマブ抵抗性のメカニズムに関与している可能性がある）

２０２５年 3 月

北　海　道　大　学

許　哲　源

(Hsu Che-Yuan)

学　位　論　文

PTEN loss is a possible mechanism of trastuzumab resistance in extramammary Paget disease

（PTEN 欠失は乳房外 Paget 病においてトラスツズマブ抵抗性のメカニズムに関与している可能性がある）

２０２５年 3 月

北　海　道　大　学

許　哲　源

(Hsu Che-Yuan)

Table of Contents

Publication and conference presentation

Part of this research was published in the following journal.

Che-Yuan Hsu, Teruki Yanagi, Takuya Maeda, Hiroshi Nishihara, Takeru Funakoshi, Kodai Miyamoto, Ririko Iwamoto, Kenzo Takahashi, Hideyuki Ujiie

Establishment of a trastuzumab-resistant extramammary Paget disease model: loss of PTEN as a potential mechanism

British Journal of Cancer. 2024 Sep;131(5):944-953.

Part of this research was presented at the following academic conferences.

Che-Yuan Hsu, Teruki Yanagi, Takuya Maeda, Hiroshi Nishihara, Kodai Miyamoto, Ririko Iwamoto, Kenzo Takahashi, Hideyuki Ujiie

Loss of PTEN in the Trastuzumab-Resistant Extramammary Paget Disease Mouse Model

The 53rd Annual Meeting of The European Society for Dermatological Research (ESDR), Poster and Oral presentation, 4-7 September 2024. Lisbon, Portugal.

Abstract

Background and Purpose

Extramammary Paget disease (EMPD) is a rare cutaneous intraepithelial adenocarcinoma primarily affecting the genital region in elderly patients. It is believed that malignant cells originate from apocrine glands in the epidermis and subsequently invade the dermis. Typically diagnosed as carcinoma *in situ*, EMPD has a favorable prognosis when treated with wide local resection. However, prognosis worsens significantly in cases with metastasis. Current treatment options for advanced EMPD, such as docetaxel monotherapy and low-dose 5-fluorouracil/cisplatin combinations, demonstrate limited effectiveness, highlighting the urgent need for innovative systemic therapies to improve clinical outcomes.

Human epidermal growth factor receptor 2 (HER2), a receptor tyrosine kinase encoded by the *ERBB2* gene on chromosome 17q12, is implicated in the progression of EMPD. Research has focused on the HER2-PI3K/MAPK signaling pathways due to the similarity of EMPD's Paget cells to those in Paget's disease of the breast. Approximately 90% of EMPD patients show no significant differences in HER2 protein overexpression or *ERBB2* gene amplification between primary tumors and lymph node metastases, suggesting HER2's role in the pathogenesis of metastasis. While trastuzumab, an HER2-targeted therapy, has improved outcomes in HER2-positive breast cancers, acquired resistance remains a significant challenge in metastatic cases. In EMPD, HER2 overexpression ranges from 15% to 65%. Notably, an EMPD patient with the *ERBB2* S310F mutation exhibited acquired resistance to trastuzumab, indicating the necessity for further research into overcoming treatment resistance and developing effective therapies for this aggressive cancer.

In this study, my purpose is to establish an innovative trastuzumab-resistant (TR) EMPD-PDX model, explore the underlying mechanisms of trastuzumab resistance, and evaluate the potential antineoplastic effects of various treatments for TR EMPD tumors.

Materials and Methods

A patient-derived xenograft (PDX) model of EMPD harboring the *ERBB2* S310F mutation was established, following a previous methodology. Tissues from a 78-year-old female patient, whose primary lesion had been excised 12 years earlier, were used to establish this model. Initially, surgically resected tissue from the patient was implanted into non-obese diabetic/severe combined immunodeficient (NOD/SCID) mice, resulting in the formation of a tumor nodule exceeding 10 mm in diameter within five months. The EMPD-PDX tumors exhibited similar morphology and protein expression to the patient's

original tumor and metastatic lymph nodes. Once the tumor reached 500 to 1000 mm^3, it was transplanted into subsequent generations, consistently retaining the pathogenic *ERBB2* mutations. In a subsequent phase of the study, an EMPD-PDX model with acquired trastuzumab resistance was developed. EMPD tumors were implanted into the lateral flanks of NOD/SCID mice and treated with escalating doses of trastuzumab over two months. Tumor volume was monitored bi-weekly, and upon exceeding 1000 mm^3, the tumors were advanced to the next generation. Resistance was further induced through continuous trastuzumab treatment for an additional eight weeks, with serial passaging resulting in a TR strain.

Genomic DNA was extracted from both trastuzumab-sensitive (TS) and TR EMPD-PDX tumors, with quality assessed via NanoDrop and electrophoresis. Targeted amplicon exome sequencing was performed on 160 cancer-related genes using the Illumina MiSeq platform, ensuring sufficient DNA quality. Data analysis utilized the GenomeJack bioinformatics pipeline.

For total RNA extraction, tumor samples were homogenized, and RNA was reverse transcribed into cDNA for quantitative PCR analysis using specific primers for genes *PTEN* and *CDH1*, normalizing results against *GAPDH*.

Antibodies for immunoblotting and immunohistochemistry were sourced from various suppliers, and protein lysates underwent SDS-PAGE followed by transfer to PVDF membranes.

The Allred scoring system was employed for quantifying FOXA1 expression in histopathological analyses, using formalin-fixed, paraffin-embedded sections from both TS and TR tumors.

Results

Tumors carrying the *ERBB2* S310F mutation were propagated in NOD/SCID mice over several generations. These tumors, implanted into the lateral flanks of mice, were subjected to escalating doses of trastuzumab to induce resistance, with tumor growth monitored regularly. When tumors exceeded 1000 mm^3, they were harvested, propagated to subsequent generations, and drug resistance was induced through continuous trastuzumab treatment.

Genetic profiling was conducted on TS and TR tumors. TR tumors exhibited a loss of *PTEN* and *CDH1* genes, accompanied by reduced mRNA expression and diminished PTEN protein levels. These findings were confirmed by histological and immunohistochemical analyses, which showed a significant reduction in PTEN protein expression in TR tumors. Further immunoblotting demonstrated an inverse correlation

between PTEN expression and the activation of the Akt pathways, as well as the downregulation of p27.

We then explored different treatment strategies for the TR EMPD-PDX model. HER2-targeted therapies were tested, with lapatinib demonstrating a marked inhibition of tumor growth, while trastuzumab had no effects in TR tumors. Cyclin-dependent kinase 4/6 inhibitors, abemaciclib and palbociclib, showed significant efficacy in suppressing tumor growth. Cytotoxic chemotherapy, including eribulin and docetaxel, proved highly effective, with a single dose of trastuzumab deruxtecan (T-DXd) leading to complete tumor eradication and no relapse over 14 days.

PTEN inhibitors BpV(HOpic) or SF1670 were administered with trastuzumab in TS EMPD-PDX models. The results showed that while trastuzumab effectively suppressed tumor growth in TS models, the addition of PTEN inhibitors partially restored the effect of trastuzumab resistance, suggesting that PTEN loss plays a significant role in the development of drug resistance.

Moreover, we investigated a clinical case of a 73-year-old Japanese male patient treated with trastuzumab plus docetaxel, whose treatment became less effective over time. Immunohistochemical analysis of biopsies taken before and after chemotherapy revealed no significant changes in PTEN or E-cadherin expression, suggesting that additional mechanisms, aside from PTEN loss, may contribute to trastuzumab resistance in clinical settings.

Discussion

Prior studies have shown that HER2 overexpression in EMPD correlates with *ERBB2* mutations, with some patients responding to anti-HER2 treatments. However, the development of acquired resistance remains a challenge, as indicated by consistent PTEN loss in our model and their prevalence in Cowden syndrome, which predisposes individuals to various malignancies. PTEN is commonly associated with trastuzumab resistance in breast cancer, and EMPD resembles Paget's disease of the breast. Our TR EMPD-PDX model constantly displayed PTEN loss, affirming their role in resistance mechanisms not only in breast cancer but also in EMPD.

The study also explored the effects of targeted therapies and cytotoxic agents in TR EMPD-PDX models. Lapatinib showed effectiveness in patients with low PTEN tumors. CDK4/6 inhibitors, abemaciclib and palbociclib, demonstrated partial tumor growth suppression. Docetaxel, eribulin, and T-DXd exhibited high efficacy against TR EMPD-PDX tumors, indicating potential treatment options despite trastuzumab resistance.

Conclusion

Our study successfully established a TR EMPD-PDX model that mirrors the characteristics of naïve tumors, particularly in terms of HER2 expression and PTEN loss. This model underscores the critical role of PTEN loss in driving TR in EMPD. We also demonstrate the potential of various therapeutic strategies. These findings suggest that targeted interventions addressing the underlying resistance mechanisms may significantly enhance treatment efficacy and outcomes for patients with TR EMPD.

Abbreviation list

The following abbreviations are used in the text and figures:

BSA	bovine serum albumin
DIN	DNA integrity number
DMSO	dimethylsulfoxide
ERK	extracellular signal-regulated kinase
EMPD	extramammary Paget disease
H&E	hematoxylin and eosin
HER2	human epidermal growth factor receptor 2
HR	hormone receptor
IHC	immunohistochemical
IACUC	Institutional Animal Care and Use Committee
LOF	loss of function
NOD/SCID	nonobese diabetic/severe combined immunodeficient
p27	$p27^{Kip1}$
PDX	patient-derived xenografts
Akt	protein kinase B
PVDF	polyvinylidene difluoride
SD	standard deviation
TBS-T	Tris-buffered saline with Tween 20
T-DXd	trastuzumab deruxtecan
TR	trastuzumab-resistant
TS	trastuzumab-sensitive

Introduction

About extramammary Paget disease

Extramammary Paget disease (EMPD), a rare cutaneous intraepithelial adenocarcinoma, is usually found in the genital region of elderly patients (Figure 1 and 2) (Ghazawi et al. 2021; Maeda et al. 2020). The malignant cells are believed to originate from apocrine glands in the epidermis and subsequently infiltrate into the dermis (Cohen, Granter, and Werchniak 2015). Typically, EMPD cases are diagnosed as carcinoma in situ, which obtain relatively favorable prognoses with wide local resection. However, the prognosis deteriorates in patients with metastasis. Various chemical regimens, such as docetaxel monotherapy and low-dose 5-fluorouracil/cisplatin combined therapy, have been proposed for advanced EMPD patients, but their effectiveness remains unsatisfactory (Ishizuki and Nakamura 2021). Managing invasive EMPD proves challenging with cytotoxic agents and radiation therapy, highlighting the need for new systemic therapies to improve clinical outcomes.

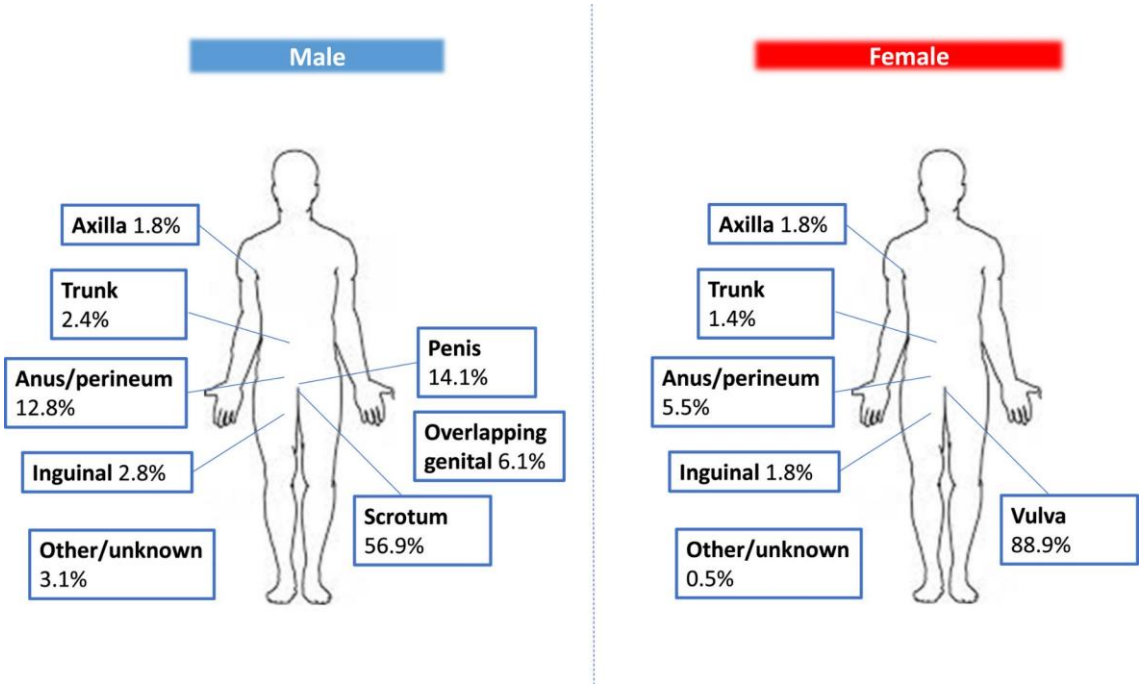

Figure 1. Illustrative depiction of the main anatomical sites affected by extramammary Paget's disease in both males and females (Ghazawi et al. 2021). In males, the primary sites for EMPD development were most commonly the scrotum (56.9%) and the penis (14.1%), while in females, the vulva was the predominant site (88.9%).

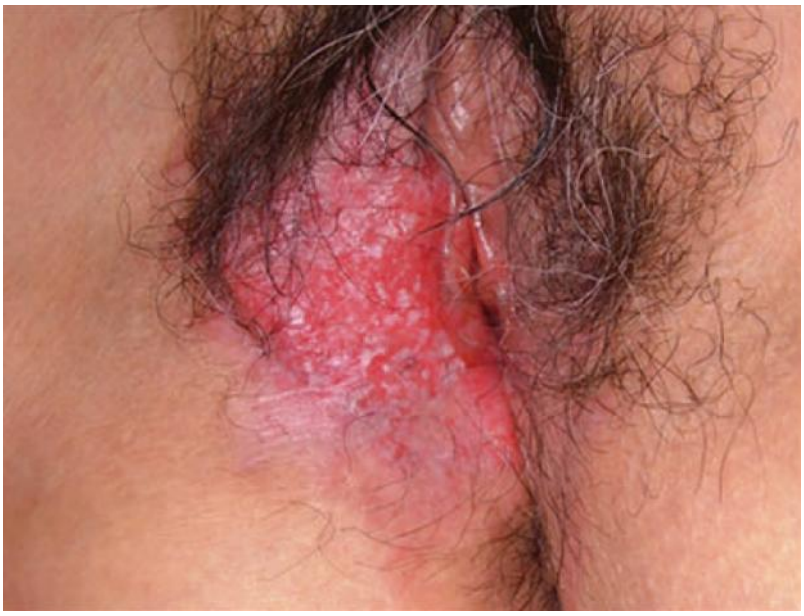

Figure 2. The clinical manifestations observed at the primary site of extramammary Paget's disease (Maeda et al. 2020). A clinical photograph displaying the primary tumor site of the patient.

About Human epidermal growth factor receptor 2

Human epidermal growth factor receptor 2 (HER2), a 185-kDa receptor tyrosine kinase, is encoded by the *ERBB2* gene located on chromosome 17q12 (Figure 3) (Cho et al. 2003). Studies on EMPD have focused on investigating the HER2-PI3K/MAPK signaling axes, given their distinctive Paget cells that resemble those in mammary Paget's disease, together with the successful clinical targeting of abnormal receptor tyrosine kinase pathways in breast cancer. Upon activation, HER2 initiates downstream PI3K and MAPK signaling cascades and contributes to EMPD progression (Figure 4) (Fukuda and Funakoshi 2018). In addition, around 90% of patients exhibit no apparent difference in HER2 protein overexpression and *ERBB2* gene amplification between primary tumors and lymph node metastases (Tanaka et al. 2016). This implies that HER2 is involved in the pathogenesis and exacerbation of a subset of metastatic EMPD, suggesting the potential disruption of both primary and metastatic tumors through HER2 blockade.

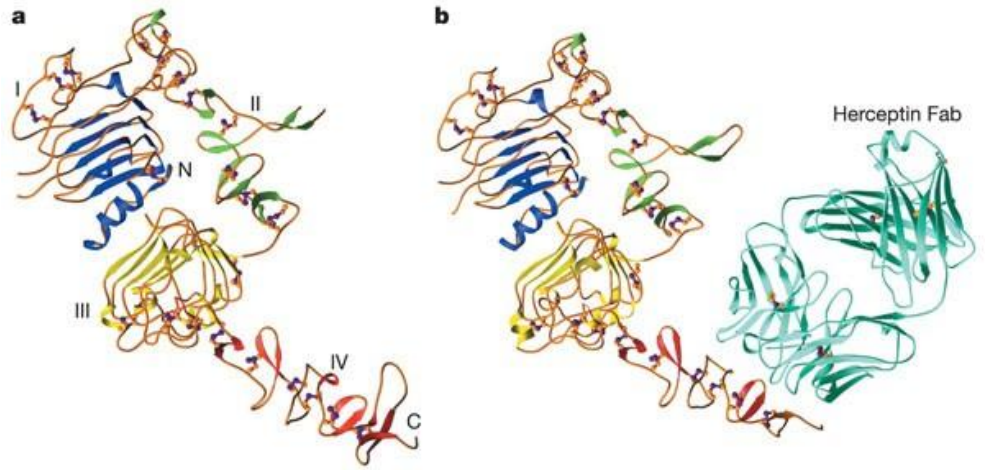

Figure 3. The structure of rat and human sHER2 (Cho et al. 2003). a. Ribbon diagram of rat sHER2, showing domains I (blue), II (green), III (yellow), and IV (red), with amino and carboxy termini indicated. Disulfide bonds are represented in purple and gold. **b.** Ribbon diagram of the human sHER2 (colored as in a) in complex with Herceptin Fab (cyan).

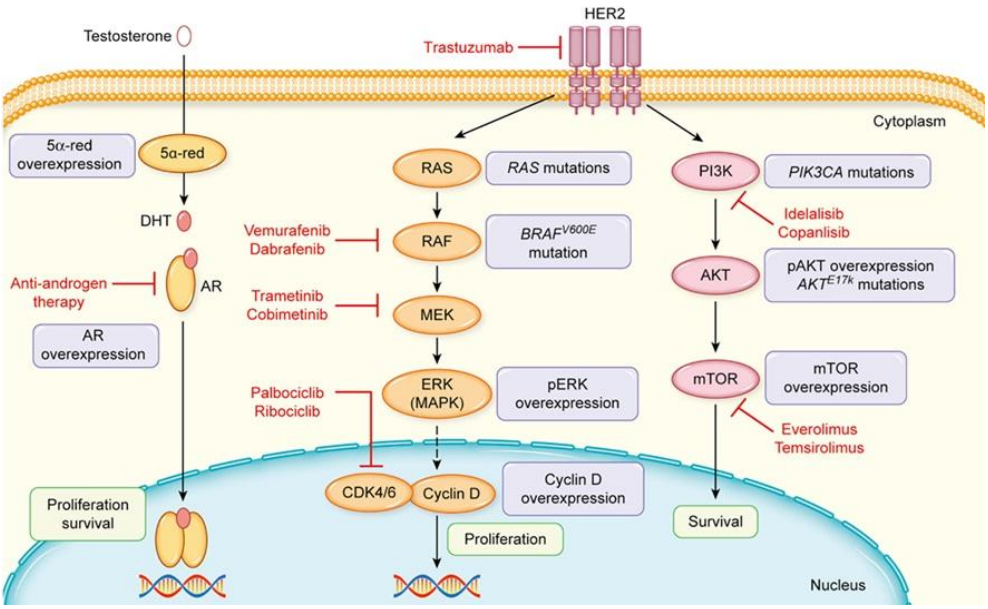

Figure 4. Signaling pathways involved in the progression of extramammary Paget's disease (Fukuda and Funakoshi 2018). The aberrant activation of HER2, along with molecules involved in the RAS–RAF–MEK–ERK or PI3K–AKT–mTOR signaling pathways, promotes the proliferation and survival of Paget cells. Similarly, the androgen–androgen receptor (AR) signaling pathway can drive Paget cell proliferation and survival. Drugs in red indicate FDA-approved treatments for other cancers that target components of these pathways.

About trastuzumab and acquired resistance

HER2-overexpressing breast cancers have long been considered among the most aggressive subtypes, associated with poor prognoses. However, the reliance of these tumors on HER2, along with the development of effective HER2-targeted therapies such as trastuzumab, pertuzumab, and more recently tucatinib and trastuzumab deruxtecan, has significantly improved survival outcomes for patients with HER2-positive breast cancer (Figure 5) (Giordano et al. 2022; Swain, Shastry, and Hamilton 2023). Currently, survival rates for early-stage HER2-positive breast cancer treated with chemotherapy and dual antibody therapy surpass 90% (von Minckwitz et al. 2017). Despite these advances, metastatic HER2-positive tumors inevitably develop resistance (Figure 6) (Z.H. Wang et al. 2022), resulting in disease progression.

The prevalence of HER2 overexpression in EMPD is reported to range from 15 to 65% (Zhu and Lewis 2022). Trastuzumab, sanctioned as a primary treatment for HER2-positive solid tumors such as gastric cancer (Smyth et al. 2020) and breast cancer (Marty et al. 2005; Z.H. Wang et al. 2022), has been employed in the management of unresectable EMPD cases. Notably, Nordmann et al. identified an EMPD patient with the *ERBB2* S310F mutation exhibiting acquired resistance to trastuzumab, potentially attributable to emerging genomic alterations (Nordmann et al. 2019). This introduces a new challenge in addressing trastuzumab resistance in EMPD patients. For preclinical models, we previously established an EMPD patient-derived xenograft (PDX) model harboring a pathogenic *ERBB2* S310F mutation, demonstrating responsiveness to anti-HER2 therapy and cytotoxic agents (Maeda et al. 2020).

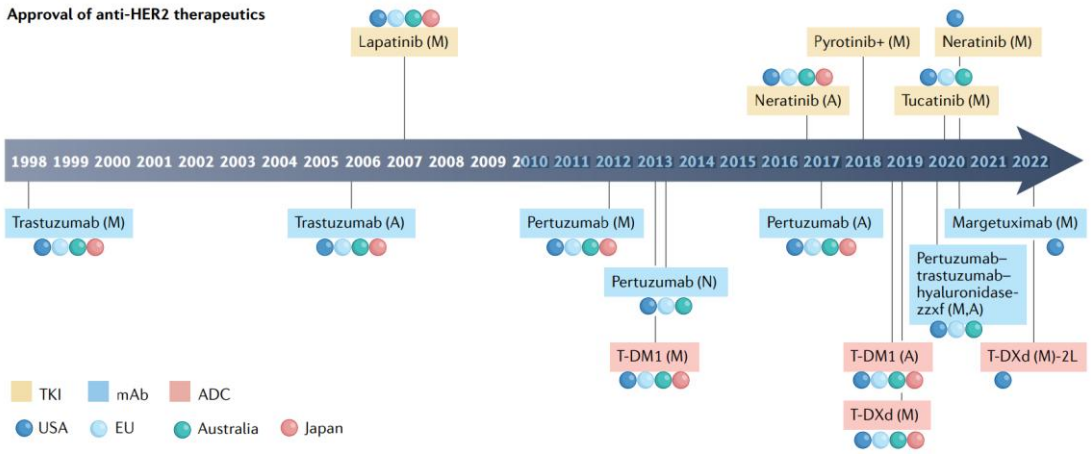

Figure 5. Advancement of HER2 as a biomarker and therapeutic target in breast cancer treatment (Swain, Shastry, and Hamilton 2023). Timeline of key preclinical discovery milestones in HER2 biology and regulatory approvals for anti-HER2 therapies. A: adjuvant setting; M: metastatic setting; N: neoadjuvant setting; +: approved in China only.

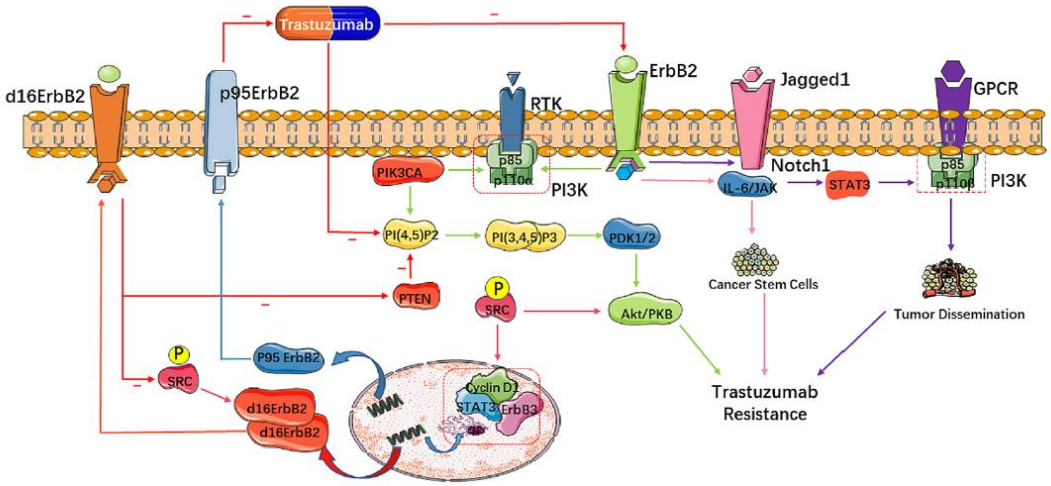

Figure 6. Molecular mechanisms of trastuzumab resistance in HER2-positive breast cancer (Z.H. Wang et al. 2022). Molecular mechanisms of trastuzumab resistance in HER2-positive breast cancer primarily involve mutations that affect cell signaling and proliferation, thereby reducing the efficacy of trastuzumab. Alterations in HER2 that impact downstream pathways diminish the drug's pharmacologic effects. For example, the truncated p95-HER2 variant, which lacks the extracellular domain necessary for trastuzumab binding, is associated with poor therapeutic response. Additionally, the d16-HER2 variant, formed by exon 16 skipping in ERBB2, creates activated d16-HER2 homodimers on the tumor cell surface, which subsequently activate SRC kinase, driving cell proliferation and tumorigenesis.

This study presents a TR EMPD-PDX model that reproduces the cell morphology and HER2 expression of naïve EMPD xenografts. Based on clinical and experimental findings, we hypothesize that targeted therapy and cytotoxic treatment, excluding trastuzumab, could remain effective against TR EMPD. Our investigation delved into potential resistance mechanisms in the TR EMPD-PDX model and evaluated diverse therapeutic strategies.

Materials and Methods

Establishment of the EMPD-PDX harboring an *ERBB2* S310F mutation (Maeda et al. 2020)

A schematic of the previous study is presented in Figure 7. To establish a patient-derived EMPD xenograft, surgically resected tissue from the patient was transplanted onto the flanks of non-obese diabetic/severe combined immunodeficient (NOD/SCID) mice. Over 5 months, the transplanted EMPD tissue developed into a firm nodule exceeding 10 mm in diameter (generation 0: G0). The EMPD-PDX tissue displayed morphology and protein expression patterns similar to those of the patient's tissues, including the primary tumor and metastatic lymph node. Once the tumor volume reached 500 to 1000 mm^3, the EMPD-PDX tumors were transplanted into the next generation of NOD/SCID mice. The EMPD-PDX tumors consistently preserved the pathogenic genomic DNA alterations of *ERBB2* (c.929C>T, p.S310F), which was also observed in the patient's metastatic lymph node. The *ERBB2* S310F mutation remained conserved across subsequent passages. Sanger sequencing of the *ERBB2* mutation confirmed that the patient's primary tumor carried the same *ERBB2* S310F mutation.

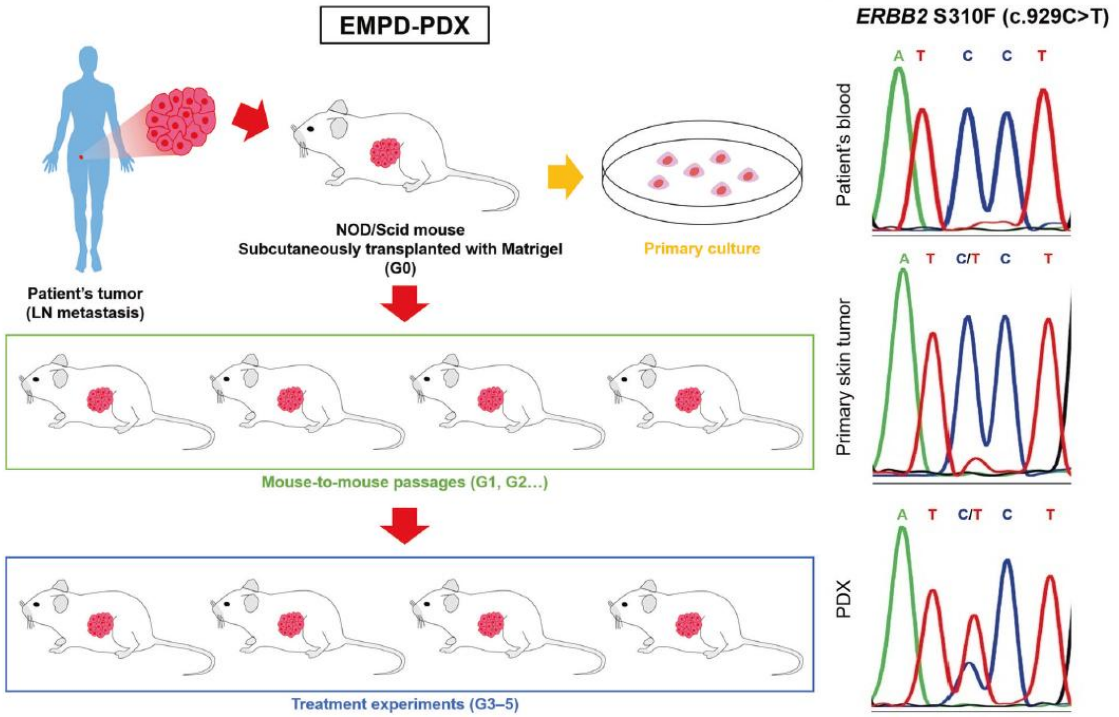

Figure 7. Schematic illustration of the establishment of the EMPD-PDX harboring an *ERBB2* S310F mutation (Maeda et al. 2020). Tissue from the EMPD patient was initially transplanted into NOD/SCID mice (generation 0: G0), with the xenografted tumors subsequently passed onto successive generations. Deep sequencing using a comprehensive cancer panel identified actionable genetic alterations in both the patient's samples and the EMPD-PDX tumors. The same gene alteration (*ERBB2* p.S310F) was found in the original patient's tumor samples (lymph node metastasis: LN) and the PDX models.

Establishment of trastuzumab-resistant EMPD-PDX mouse model

A schematic of the current study is shown in Figure 8. The EMPD tissues were collected from inguinal lymph node metastases in a 78-year-old Japanese female, whose primary genital skin lesion had been excised 12 years prior to the occurrence of lymph node metastasis. The naïve tumor was subsequently propagated and maintained in the NOD/SCID mice for several generations (Maeda et al. 2020). In this study, the primary objective was to develop an EMPD-PDX model with acquired trastuzumab resistance. The EMPD tumors were implanted into the lateral flanks of NOD/SCID mice (G0). These mice received weekly intraperitoneal injections of trastuzumab with a gradually increasing dose (2→4→8→12→16→20 mg/kg, Herceptin®, Chugai Pharmaceutical Co., Ltd., Tokyo, Japan) over 2 months (Irie et al. 2020). Tumor volume was calculated using the formula (long axis × short axis^2)/2 and was measured twice per week (Yanagi et al. 2014). When the tumors reached a size exceeding 1000 mm^3, the mice were advanced to the G1 generation. Then, resistance was induced through intraperitoneal injections of trastuzumab (10-20 mg/kg) for an additional 8 weeks. Xenografts that maintained an optimal size above 1000mm^3 were serially passaged to the G2 generation, which we define as a TR strain.

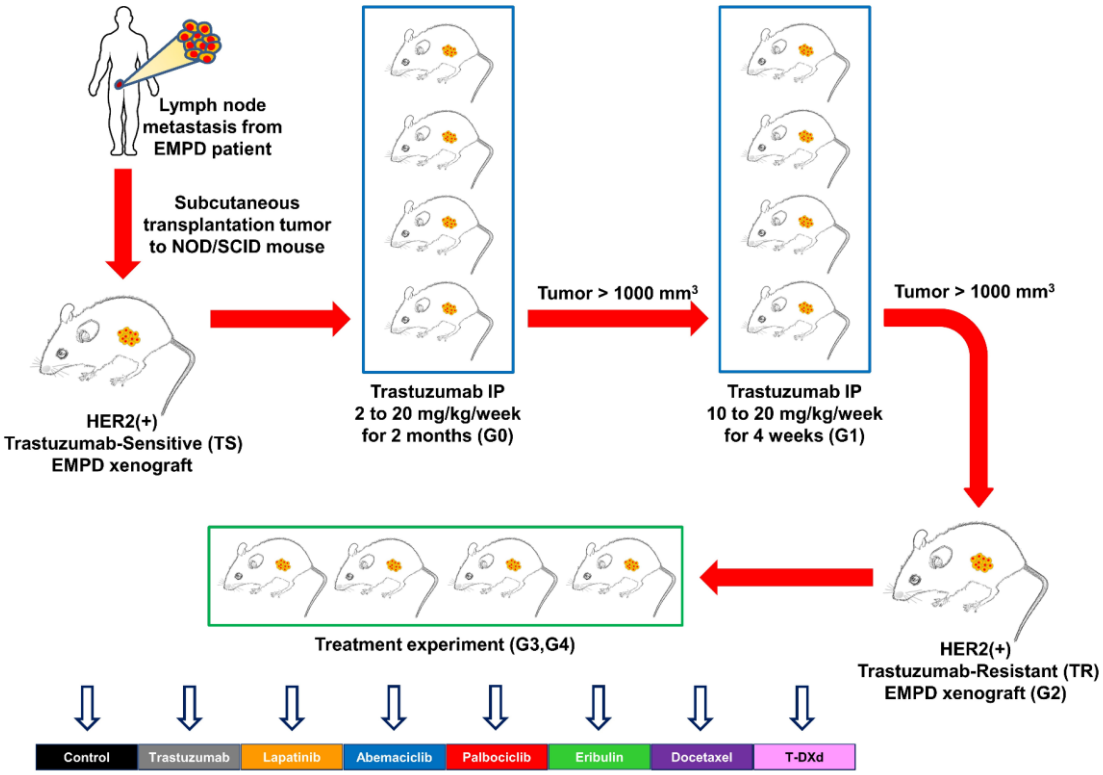

Figure 8. Schematic illustration of the establishment of the trastuzumab-resistant EMPD-PDX mouse model and the treatment experiment. Enlarged tumors sensitive to trastuzumab (TS) were transplanted into NOD/SCID mice (G0) to develop trastuzumab-resistant (TR) EMPD xenografts. During G0 generation, these mice were injected with trastuzumab (with a gradual increase in dose from 2→4→8→12→16→20 mg/kg) intraperitoneally every week over 2 months. Once the tumor grew larger than 1000 mm^3 in size, it was then propagated to the G1 generation. Resistance was subsequently induced via intraperitoneal injection of trastuzumab (10 to 20 mg/kg) for another 8 weeks. The xenografts that were able to maintain an optimal size over 1000 mm^3 were serially passaged to the G2 generation, which we define as a TR strain. In treatment experiments (G3, G4), tumor-bearing NOD/SCID mice were randomized into the control group, trastuzumab group, lapatinib group, abemaciclib group, palbociclib group, eribulin group, docetaxel group, and the trastuzumab deruxtecan (T-DXd) group.

Gene mutation analysis

Genomic DNA was isolated from the TS and TR EMPD-PDX tumors using the DNA Mini Kit (51304, QIAGEN, Hilden, Germany). The concentration and purity of the DNA samples were assessed with a NanoDrop 2000c Spectrophotometer (Thermo Fisher, MA, USA), and DNA fragment integrity was verified through electrophoresis on a 1% agarose gel. DNA sample concentrations were standardised to 20 ng/μL and stored at −30 °C until needed.

Genomic testing was carried out at the genomic unit of the Keio Cancer Center in Tokyo, Japan. The DNA quality was initially evaluated based on the DNA Integrity Number (DIN) score, calculated using the Agilent 2000 TapeStation system (Agilent Technologies, CA, USA). Subsequently, targeted amplicon exome sequencing was performed on 160 cancer-related genes using the MiSeq sequencing platform (Illumina, CA, USA). The list of these 160 cancer-related genes can be found in Table 1. The minimum requirement for DNA was 50 ng, and the DNA needed to have a DIN score exceeding 3.1 to be considered of sufficient quality. Sequencing data analysis was conducted using an in-house bioinformatics pipeline known as GenomeJack (Mitsubishi Space Software, Tokyo, Japan) (Maeda et al. 2020).

Table 1. Next-generation sequencing-based multiplex gene assay (PleSSision-160)

ABL1	AKT1	AKT2	ALK	AMER1	APC	AR	ARID1A
ARID2	ASXL1	ATM	ATRX	BAP1	BCL6	BCOR	BRAF
BRCA1	BRCA2	BRIP1	BTK	BUB1B	CARD11	CBL	CBLB
CD79A	CD79B	CDC73	CDH1	CDK12	CDK4	CDKN2A	CHEK2
CIC	CREBBP	CRLF2	CSF1R	CTNNB1	CYLD	DAXX	DDB2
DDR2	DICER1	DNMT3A	ECT2L	EGFR	EP300	EPCAM	ERBB2
ERBB3	ERBB4	ERCC5	ESR1	EZH2	FAM46C	FANCA	FANCD2
FANCE	FAS	FBXO11	FBXW7	FGFR2	FGFR3	FH	FLCN
FLT3	FUBP1	GATA1	GATA2	GATA3	GNA11	GNAQ	GNAS
GPC3	GRIN2A	H3F3A	HIST1H3B	HNF1A	HRAS	HSPH1	IDH1
IDH2	IKZF1	IL6ST	IL7R	JAK1	JAK2	JAK3	KDM6A
KDR	KIT	KLF6	KMT2D	KRAS	MAP2K1	MAP2K2	MAP2K4
MAP3K1	MAP4K3	MDM2	MED12	MEN1	MET	MLH1	MSH2
MSH6	MTOR	MUTYH	MYC	MYD88	NF1	NF2	NFE2L2
NFKBIA	NOTCH1	NOTCH2	NPM1	NRAS	PALB2	PAX5	PBRM1
PDGFRA	PHF6	PIK3CA	PIK3R1	PMS2	PPP2R1A	PRDM1	PRKAR1A
PTCH1	PTEN	PTPN11	RAC1	RB1	RET	ROS1	SDHB
SETD2	SF3B1	SLC7A8	SMAD4	SMARCA4	SMARCB1	SMO	SPOP
SRC	STK11	SUFU	TERT	TNFAIP3	TNFRSF14	TP53	TSC1
TSC2	TSHR	U2AF1	VHL	WT1	XPC	ZNF2	ZRSR2

Total RNA extraction and qRT-PCR analysis

TS and TR EMPD-PDX tumors were ground and homogenized in an appropriate amount of Buffer RLT Plus using the RNeasy Plus Mini Kit (Qiagen), and total RNA was isolated from the lysates. RNA concentrations were measured using NanoDrop 2000c Spectrophotometer, and the samples were stored at -80°C until use. RNA was reverse transcribed into cDNA using SuperScript IV VILO MasterMix (11755-050, Thermo Fisher). A total of 1.0 μg of isolated RNA was combined with 1 μL of 10× ezDNase Buffer, 1 μL of ezDNase enzyme, and Nuclease-free water to a final volume of 10 μL, then mixed gently. The mixture was incubated at 37°C for 2 minutes, transferred to ice, and then 4 μL of SuperScript IV VILO MasterMix and 6 μL of Nuclease-free water were added. The mixture was gently mixed and incubated at 25°C for 10 minutes, followed by 50°C for 10 minutes, and terminated at 85°C for 5 minutes. The cDNA was stored at -20°C.

Next, cDNA expression was analyzed using the SYBR Green System (Takara Bio Inc., Shiga, Japan). The PCR reaction mixture was prepared as shown below.

Reagent	Vol.
TB Green Premix Ex Taq II (Tli RNaseH Plus) (2 ×)	10 μL
PCR Forward Primer (10 μM)	0.8 μL
PCR Reverse Primer (10 μM)	0.8 μL
ROX Reference Dye (50 ×)	0.4 μL
Template cDNA (＜100 ng)	2 μL
distilled water	6 μL
Total	20 μL

After thoroughly mixing the reagents and ensuring they were homogeneous, PCR reactions were carried out using the following standard shuttle PCR protocol. The detection instrument used was the StepOnePlus Real-Time PCR System (Thermo Fisher).

Stage 1：Initial denaturation
Reps：1
95℃ for 30 sec
Stage 2：PCR reaction
Reps：40
95℃ for 5 sec
60℃ for 30 sec
Stage 3：Melt Curve stage

After the reaction was completed, the amplification curve and melting curve were checked, and a calibration curve was created for quantification. The sequences of primers specific to human gene PTEN and CDH1 and the control gene GAPDH are shown in Table 2. The PTEN and CDH1-specific primers for real-time PCR were designed using the Roche Assay Design Center (https://diagnostics.roche.com/us/en/products/product-category/assay-offerings.html) (Shen et al. 2006; Malathi Veeramani 2022). All experiments were performed in duplicate, and the samples were normalized and compared using the GAPDH values from trastuzumab-sensitive EMPD-PDX tumors.

Table 2. Primers for Quantitative PCR for Human *PTEN* (Shen et al. 2006), *CDH1* (Malathi Veeramani 2022), and *GAPDH*

PTEN	Forward	5’-CAAGATGATGTTTGAAACTATTCCAATG-3’
	Reverse	5’-CCTTTAGCTGGCAGACCACAA-3’
CDH1	Forward	5’-CAGCACGTACACAGCCCTAA 3’
	Reverse	5'-ACCTGAGGCTTTGGATTCCT 3’
GAPDH	Forward	5'-GAAGGTGAAGGTCGGAGTC-3'
	Reverse	5'-ATGGGATTTCCATTGATGAC-3'

Reagents and antibodies

The following items were purchased from the indicated sources: antibodies against E-cadherin (diluted at 1:1000 in 5% non-fat dry skim milk (FJ198-10605, Wako Pure Chemical Industries, Ltd, Osaka, Japan) in Tris-buffered saline with Tween 20 (TBS-T, sc-21791, Santa Cruz Biotechnology, Inc., TX, USA)), PTEN (diluted at 1:1000 in 5% non-fat dry skim milk in TBS-T, #9559, Cell Signaling, MA, USA), phospho-Akt (diluted at 1:1000 in 5% bovine serum albumin (BSA) in TBS-T, #4060, Cell Signaling), Akt (diluted at 1:1000 in 5% non-fat dry skim milk in TBS-T, #4691, Cell Signaling), phospho-ERK (diluted at 1:1000 in 5% BSA in TBS-T, #9101, Cell Signaling), ERK (diluted at 1:1000 in 5% non-fat dry skim milk in TBS-T, #4695, Cell Signaling), p27 (diluted at 1:1000 in 5% non-fat dry skim milk in TBS-T, #2552, Cell Signaling), β-actin (diluted at 1:2000 in 5% non-fat dry skim milk in TBS-T, #A5441, Sigma-Aldrich, MO, USA), HRP-linked horse anti-mouse IgG secondary antibody (diluted at 1:5000 in TBS-T, #7076, Cell Signaling), and HRP-linked goat anti-rabbit IgG secondary antibody (diluted at 1:5000 in TBS-T, #7074, Cell Signaling). Matrigel (#356234) was purchased from BD Biosciences, NJ, USA.

SDS-PAGE and immunoblotting

Tumor tissues were washed by PBS twice and homogenized in RIPA buffer (50 mM Tris pH 7.5, 150 mM NaCl, NP40 1%, sodium deoxycholate 0.5%, SDS 0.1%, NaF, final concentration 1 nM, NaV_3O_4, final concentration 10 μM., 188-02453, Wako) with the addition of a protease inhibitor cocktail (cOmplete™ Mini, Roche, Basel, Switzerland) and a phosphatase inhibitor cocktail (PhosSTOP™, Roche). The tumor lysates were collected in 1.5 mL Eppendorf tubes. After centrifugation at 15,000 rpm for 10 minutes at 4°C, the supernatant was collected and transferred to a new Eppendorf tube. NuPAGE LDS Sample Buffer (lithium dodecyl sulfate, pH 8.4, Invitrogen, MA, USA) and NuPAGE Sample Reducing Agent (500 mM dithiothreitol, 10× ready-to-use concentration, Invitrogen) were added and mixed. The mixture was then boiled at 70°C for 10 minutes.

The resulting lysates were separated using NuPAGE™ Bis-Tris protein gels (4-12% gradient, Invitrogen) with Precision Plus Protein Standards marker (#161-0374, Bio-Rad, CA, USA). Electrophoresis was performed using MOPS SDS Running Buffer (#1908733, Life Technology, CA, USA). The separated protein was then transferred from the gel to polyvinylidene difluoride membranes (iBlot™ 2 PVDF Transfer Stacks, Invitrogen). Blocking incubation were conducted in TBS-T with either 5% non-fat dry skim milk or 5% BSA for 60 minutes at room temperature with shaking.

The primary antibody was added, and the antigen-antibody reaction was allowed to proceed for 12 to 16 hours with shaking at 4°C. After three 20-minute washes with TBS-T, the reaction was continued at room temperature for 60 minutes using HRP-labeled horse anti-mouse IgG antibody and HRP-labeled anti-rabbit IgG antibody (both from Cell Signaling Technology) as secondary antibodies. Following another three washes with TBS-T, the PVDF membranes were incubated for approximately 1 minute in a mixture of 500 µL of Luminol Enhancer Solution and 500 µL of Peroxide Solution (ECL™ Prime Western Blotting Detection Reagent, Cytiva, Amersham, UK). Images were captured using the ImageQuant LAS4000 system (GE Healthcare, IL, USA) and quantified by the ImageJ software application (developed by Wayne Rasband; available at https://imagej.net/ij/).

Histopathological analyses

Sections of 10% formalin-fixed (Wako), paraffin-embedded tissue from both TS and TR EMPD-PDX tumors, and a 73-year-old Japanese male EMPD patient were sliced into 4-µm sections. Hematoxylin and eosin (H&E) staining, as well as immunohistochemistry for HER2 (A0485, Dako, Denmark), E-cadherin (#3195, Cell Signaling), PTEN (#9559, Cell Signaling), and FOXA1 (ab170933, Abcam, Cambridge, UK), were performed to assess the histopathological changes in EMPD-PDX xenografts before and after repetitive trastuzumab treatments. DAB chromogen was used to produce a brown color.

The Allred scoring system (Table 3) (Allred et al. 1998), which exhibits high-level reproducibility, was chosen to quantify FOXA1 expression. This approach assigns a total score ranging from 0 to 8, which is a summation of intensity on a scale of 0 to 3 and percentage on a scale of 0 to 5. Scoring was performed by the same observer. The pattern of FOXA1 staining was assessed according to the Allred score, and the samples were categorised into two groups: positive (+, Allred score ≥ 3) or negative (−, Allred score <3).

Table 3. Allred system of scoring for ER and PR (Pyla et al. 2020; Allred et al. 1998)

Proportion Score	
Score	*Percentage of stained cells*
0	No cells are ER positive
1	≤1% cells are ER positive
2	1-10% cells are ER positive
3	11-33% cells are ER positive
4	34-66% cells are ER positive
5	67-100% cells are ER positive
Intensity Score	
Score	*Intensity of staining*
0	Negative
1	Weak
2	Intermediate
3	Strong
Allred Score (Allred score=Proportion Score + Intensity Score)	
Allred score	*Effect of hormone therapy*
0-1	No effect
2-3	Small (20%) chance of benefit
4-6	Moderate (50%) chance of benefit
7-8	Good (75%) chance of benefit

ER: Estrogen receptor; PR: Progesterone receptor

***In vivo* experiment on the trastuzumab-resistant EMPD-PDX mouse model**

Five-week-old female NOD/ShiJic-scidJcl mice were procured from CLEA Japan, Inc. The mice were housed at the Institute for Animal Experimentation of the School of Medicine at Hokkaido University for at least five days to ensure they established regular eating and sleeping patterns and adapted to the environment before being used in experiments. They were provided with sterile distilled water and standard feed ad libitum and housed in a controlled environment (22-25 °C, 12-h light/dark cycle) under specific pathogen-free conditions.

The patient-derived xenograft (PDX) experiments were conducted in accordance with our previous publication (Maeda et al. 2020). In the treatment experiments, tumor growth curves for TR EMPD-PDX (G3, G4) were generated by dynamically measuring tumor volume. Tumor-bearing NOD/ShiJic-scidJcl mice with volumes ranging from 300 to 400 mm^3 were randomly assigned to control and different treatment groups. The control group (n = 4) received weekly intraperitoneal injections of 200 μL of PBS. Trastuzumab (n = 4, 20 mg/kg) was administered intraperitoneally once per week (Maeda et al. 2020). Lapatinib (n = 4, 200 mg/kg, CS-0036, ChemScene, NJ, USA) was administered orally daily in 0.5% Methyl Cellulose (#4000, Nacalai Tesque, Kyoto, Japan) and 0.1% Tween 80 (P1754, Sigma-Aldrich) (Nonagase et al. 2016). Abemaciclib (n = 4, 50 mg/kg, LY2835219, Adooq BioScience, CA, USA) was administered orally daily in 5% dimethylsulfoxide (CultureSure® DMSO, 037-24053, Wako), 40% Polyethylene glycol 300 (PEG300, 202371, Sigma-Aldrich), 5% Tween 80, and 50% water (Patnaik et al. 2016). Palbociclib (n = 4, 120 mg/kg, PZ0383, Sigma-Aldrich, MO, USA) was administered orally daily in water (Fry et al. 2004). Eribulin (n = 4, 1.5 mg/kg, Halaven®, Eisai Co., Ltd., Tokyo, Japan) was injected into the tail vein once per week (Maeda et al. 2020). The Docetaxel group (n = 4, 20 mg/kg, #sc-201436, Santa Cruz Biotechnology, CA, USA) received intraperitoneal injections once per week (Maeda et al. 2020). The trastuzumab deruxtecan (T-DXd) group (n = 4, 10 mg/kg, Enhertu®, Daiichi-Sankyo/AstraZeneca, Tokyo, Japan) received a single intravenous dose (Tokuchi et al. 2022). Tumor volume was measured twice per week using calipers, and tumor weights were recorded 28 days after treatment initiation, all done in a blinded manner.

***In vivo* experiment on the trastuzumab-sensitive EMPD-PDX mouse model using PTEN inhibitors**

In the treatment experiments of PTEN inhibitors, tumor growth curves for TS EMPD-PDX were generated by measuring tumor volume. TS EMPD tumors obtained from the previous study (Maeda et al. 2020) were subcutaneously implanted into the lateral flanks

of NOD/ShiJic-scidJcl mice. Tumor-bearing mice with a volume range 50 to 100 mm^3 were randomly assigned to trastuzumab and two treatment groups. The trastuzumab group (n = 4) received intraperitoneal injections of trastuzumab (10mg/kg) twice per week for 14 days. In the BpV(HOpic) group (n = 4, 0.5mg/kg, HY-128693, MedChemExpress, NJ, USA), mice were intraperitoneally pretreated with BpV(HOpic) for 3 days, followed by trastuzumab (10mg/kg) twice per week and BpV(HOpic) every day for 14 days (Feng et al. 2020). In the SF1670 group (n = 4, 10 μM/kg, HY-15842, MedChemExpress), mice were intraperitoneally pretreated with SF1670 (solved in 5% DMSO, 40% PEG300, 5% Tween 80, and 50% water) for 3 days, followed by trastuzumab (10 mg/kg) twice per week and SF1670 every day for 14 days (Yue et al. 2021). Tumor volume was measured twice per week using calipers, and tumor weights were recorded 14 days after treatment initiation, all done in a blinded manner.

Ethics approval and consent to participate

The study protocol complied with the Declaration of Helsinki and was approved by the Institutional Review Board of Keio University (IRB approval number: 20110159). The 73-year-old Japanese male EMPD patient provided written informed consent prior to enrollment. The animal study protocol was approved by the Institutional Animal Care and Use Committee (IACUC) of Hokkaido University (approval number 19-0093) and the Committee on Animal Experiments of the University of the Ryukyus (approval number A2023052), and all experiments were performed in accordance with the regulations of IACUC. All methods are reported in accordance with ARRIVE guidelines (https://arriveguidelines.org) for the reporting of animal experiments under ethics approval and consent to participate.

Statistical analyses

Quantitative data is presented as the mean ± standard deviation (SD). The statistical significance of the treatment groups was assessed using the Student's *t* test to compare each category. At least three independent experiments were conducted for statistical analysis. Two-tailed statistical tests were performed, and a *P* value of less than 0.05 was considered statistically significant.

Results

Establishment of trastuzumab-resistant EMPD-PDX mouse model

The naïve tumors harboring the *ERBB2* S310F mutation were propagated and maintained in NOD/SCID mice for several generations (Maeda et al. 2020). They are now being used to develop a new EMPD-PDX model with acquired trastuzumab resistance (Figure 8 to 10).

Six fresh tumors labeled A, B, C, D, E, and M were each divided into two parts. The divided pieces are labeled accordingly (A1 and A2, B1 and B2, etc.). These tumor pieces were then implanted into the lateral flanks of NOD/SCID mice (G0) (Figure 9), with the designation indicating where they were implanted: "1" for the left flank and "2" for the right flank. These mice received weekly intraperitoneal injections of trastuzumab with a gradually increasing dose (2→4→8→12→16→20 mg/kg, Herceptin®, Chugai Pharmaceutical Co., Ltd., Tokyo, Japan) over 2 months (Irie et al. 2020).

The tumor volume was measured twice a week. Whenever the tumor volume increased for one consecutive week, the trastuzumab dosage was increased. If the tumor volume remains stable for one consecutive week, the current drug dosage is maintained. If the tumor volume decreased for one consecutive week, the drug administration was halted until the tumor resumes growth. When the tumors reached a size exceeding 1000 mm^3, the mice were sacrificed and each tumor was advanced to the G1 generation.

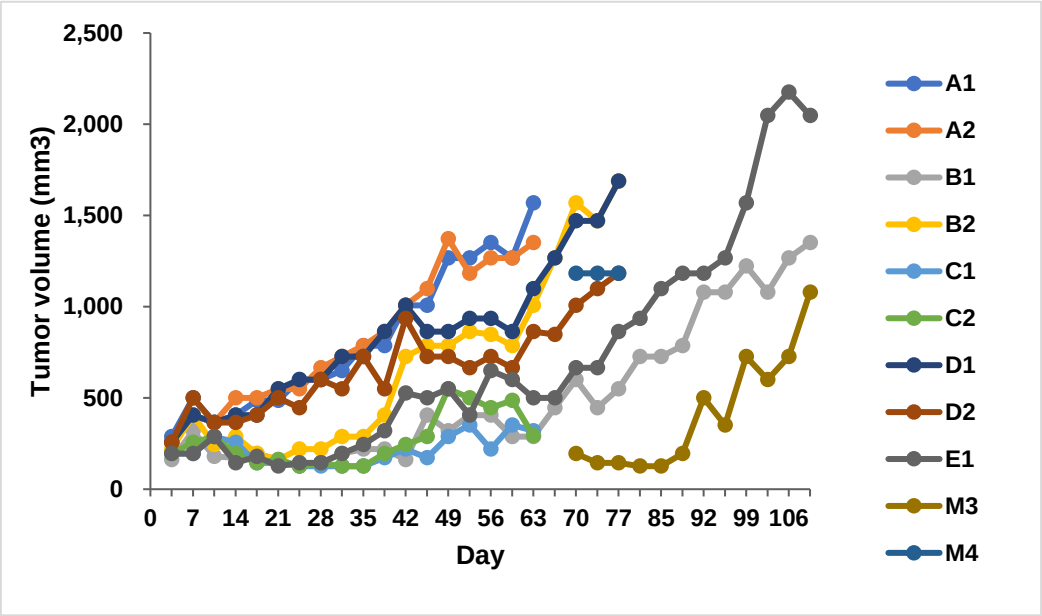

Figure 9. Tumor growth curve of the EMPD-PDX mouse model developing trastuzumab resistance in Generation 0 (G0). Each labeled tumor showed a different growth curve pattern during continuous trastuzumab treatment.

In the G0 generation, the time it took for the tumor volume to exceed 1000 mm^3 varied due to differences in growth rates. After being transplanted into the G1 generation, the tumors were categorized into three groups based on their growth speed for further monitoring (Figure 10, A to C): A: fast-growing, B: moderate-growing, and C: slow-growing. Each tumor was then divided into two halves, and these tumor pieces were then implanted into the lateral flanks of NOD/SCID mice (G1), with "1" indicating the left flank and "2" indicating the right flank. Then, resistance was induced through intraperitoneal injections of trastuzumab (10-20 mg/kg) for an additional 8 weeks. Xenografts that maintained an optimal size above $1000mm^3$ were serially passaged to the G2 generation, which we define as a TR strain.

In the following experiment, one tumor was randomly selected from each of the four groups (A, B, D, M) and designated as TR1, TR2, TR3, and TR4, respectively, for use in the subsequent experiments.

A

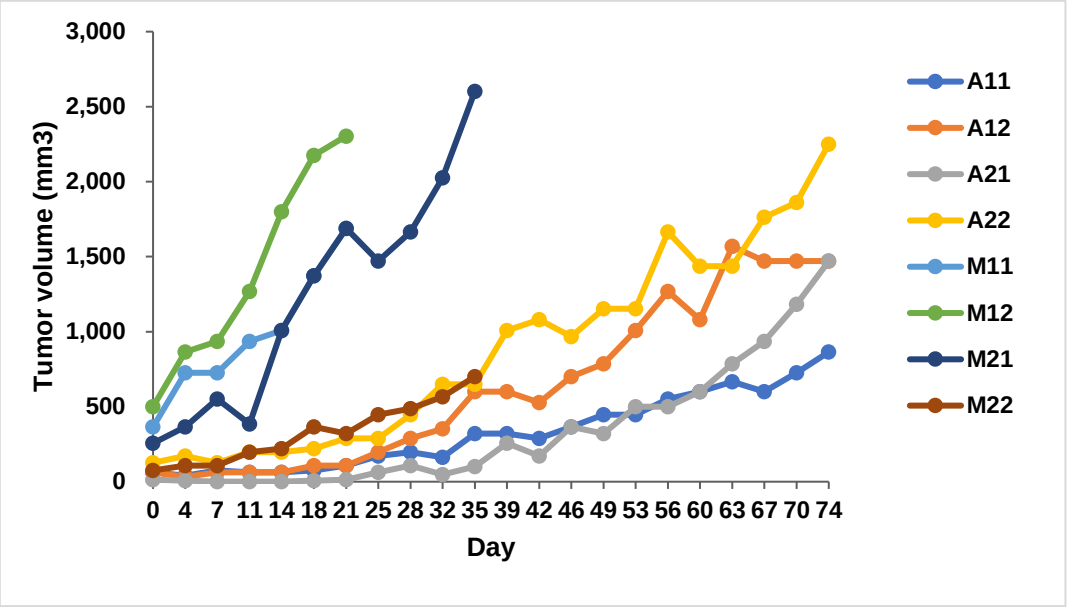
Tumor volume (mm3)
3,000
2,500
2,000
1,500
1,000
500
0
0 4 7 11 14 18 21 25 28 32 35 39 42 46 49 53 56 60 63 67 70 74
Day
A11
A12
A21
A22
M11
M12
M21
M22

B

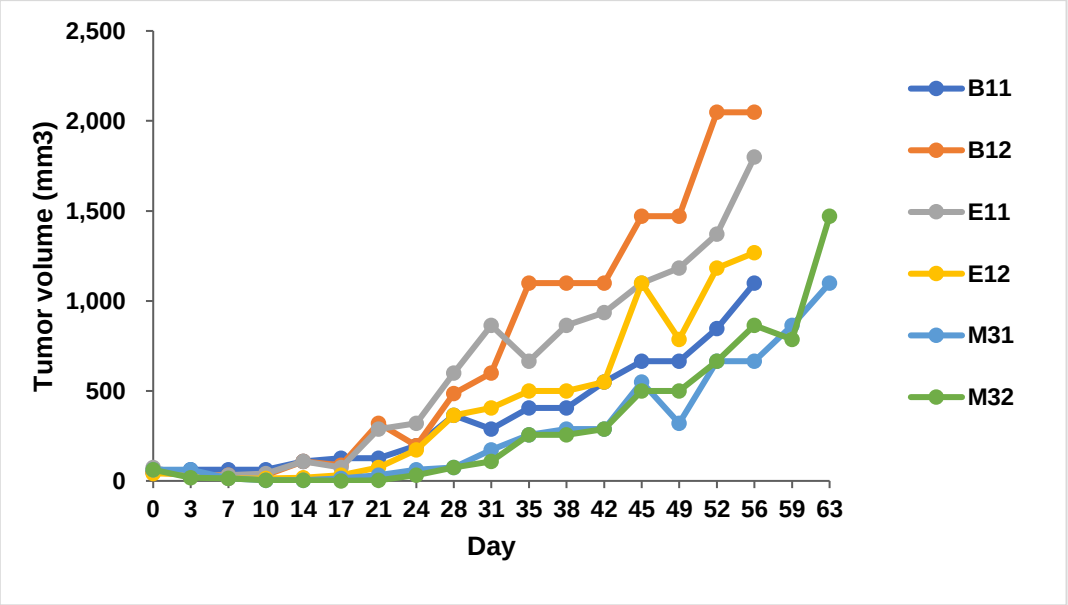
Tumor volume (mm3)
2,500
2,000
1,500
1,000
500
0
0 3 7 10 14 17 21 24 28 31 35 38 42 45 49 52 56 59 63
Day
B11
B12
E11
E12
M31
M32

C

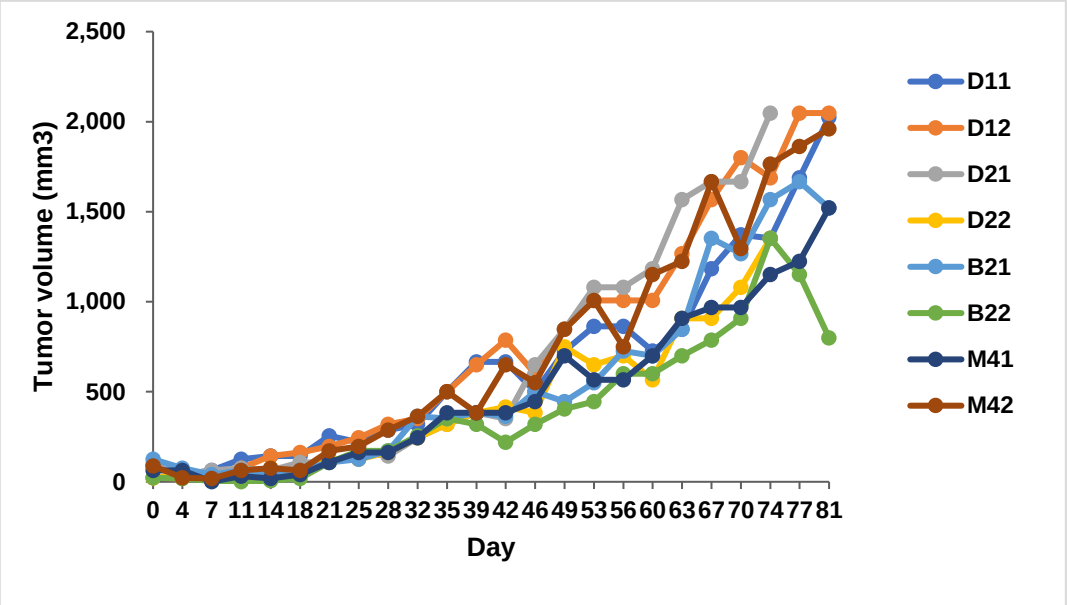

Figure 10. Tumor growth curve of the EMPD-PDX mouse model developing trastuzumab resistance in Generation 1 (G1). Fast-growing tumors from Figure 9 are categorized as (A), moderate-growing tumors as (B), and slow-growing tumors as (C). Each labeled tumor displayed a distinct growth curve pattern throughout continuous trastuzumab treatment.

Trastuzumab-resistant EMPD-PDX shows *PTEN* and *CDH1* gene deficiencies, lower RNA expression levels of *PTEN* and *CDH1*, and reduced PTEN protein levels compared to trastuzumab-sensitive tumors

To explore the genotypic and phenotypic characteristics of trastuzumab-sensitive (TS) and TR EMPD-PDX tumor cells, we carried out cancer gene profiling, mRNA expression level, histological examination, and immunoblot analyses. Initially, deep sequencing using a comprehensive cancer panel was performed to compare the cancer-associated genomic profiles of TS and TR tumors (Figure 11 and Table 4). Common mutations in *BRCA2*, *ERBB2*, *GRIN2A*, *NF1*, *RB1*, *FGFR1*, and *KMT2D* were identified in both TS and TR1 to TR4 tumors. In contrast, *CDH1* and *PTEN* genes were exclusively retained in TS xenografts, not in TR xenografts.

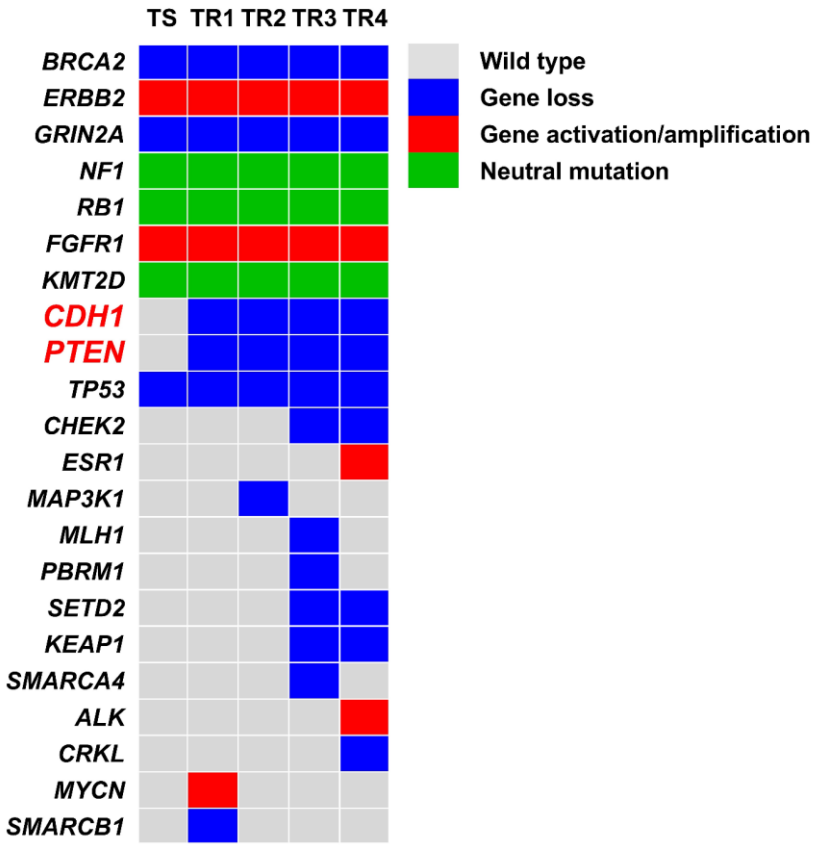

Figure 11. Comparison between trastuzumab-sensitive (TS) and several trastuzumab-resistant (TR) EMPD tumors based on the Next-generation sequencing-based multiplex gene assay (PleSSision-160). Each row symbolizes a cancer gene, and each column represents a tumor in these two groups of TS and TR EMPD-PDX mouse models. TR1 to TR4 means the extracted tumor originated from individual trastuzumab-resistant EMPD mice. "Wild type" describes alleles deemed to be normal or typical. "Gene loss" means the loss of a gene from the genome. "Gene activation/amplification" means the process of activation of genes, allowing expression, or increasing the number of copies of a gene in the genome. "Neutral mutation" means changes in DNA sequence that are neither beneficial nor detrimental to the function of a protein. The major difference between the TS and TR groups is the loss of the genes *CDH1* and *PTEN*.

Table 4. Genetic alterations for samples of trastuzumab-sensitive (TS) and several trastuzumab-resistant (TR) EMPD tumors based on the Next-generation sequencing-based multiplex gene assay (PleSSision-160).

	TS		TR1		TR2		TR3		TR4	
Gene	AA Change	VAF	AA Change	VAF	AA Change	VAF	AA Change	VAF	AA Change	VAF
BRCA2	p.R2520*	100.0	p.R2520*	99.6	p.R2520*	100.0	p.R2520*	99.3	p.R2520*	100.0
	p.L2753P	12.0							p.L2753P	5.9
ERBB2	p.S310F	52.6	p.S310F	57.0	p.S310F	52.8	p.S310F	57.3	p.S310F	61.0
GRIN2A	p.L1377=	68.1	p.L1377=	18.6	p.L1377=	12.1	p.L1377=	13.5	p.L1377=	33.6
	p.R1372G	64.8	p.R1372G	15.7	p.R1372G	9.3	p.R1372G	10.3	p.R1372G	29.9
	p.G1258=	29.5	p.G1258=	4.4					p.G1258=	7.5
	p.L98F	27.3							p.L98F	5.8
NF1	p.P1359S	20.1								
	p.D2545N	51.4	p.D2545N	47.9	p.D2545N	47.8	p.D2545N	48.7	p.D2545N	49.9
RB1	p.S780*	79.4	p.S780*	95.7	p.S780*	97.5	p.S780*	98.6	p.S780*	91.3
FGFR1	Amplification		Amplification		Amplification		Amplification		Amplification	
	p.Q122R	6.9								
	p.A107V	5.6								
	p.F76L	5.8								
	p.A69V	6.0								
KMT2D	p.G5087E	39.7	p.G5087E	45.8	p.G5087E	47.0	p.G5087E	48.6	p.G5087E	44.1
	p.G1628Vfs*94	16.7			p.G1628Vfs*94	4.1			p.G1628Vfs*94	4.6
CDH1			Loss		Loss		Loss		Loss	
									p.D538E	6.2
									p.S543F	5.7
									p.L548M	5.5
PTEN	p.T398S	100.0								
			Loss		Loss		Loss		Loss	

AA change: amino acid change

VAF (%): variant allele frequency

Table 4. (Continued)

Gene	TS		TR1		TR2		TR3		TR4	
	AA Change	VAF	AA Change	VAF	AA Change	VAF	AA Change	VAF	AA Change	VAF
TP53	p.R181C	6.3							p.R181C	8.5
	p.Q165K	51.4	p.Q165K	11.9	p.Q165K	18.1	p.Q165K	9.7	p.Q165K	23.7
			p.A161T	86.6	p.A161T	81.5	p.A161T	9.1	p.A161T	74.6
			Loss		Loss		Loss		Loss	
									p.T170P	6.5
									p.Y163F	8.1
									p.T170M	6.4
									p.M169I	6.3
CHEK2							Loss		Loss	
									p.E497D	8.6
									p.A496T	8.3
									p.R474K	14.6
									p.A258E	12.4
ESR1	p.V368G	23.3								
	p.S433C	35.5							Amplification	
MAP3K1	p.M641I	31.8								
	p.S418C	31.0								
					Loss					
MLH1	p.L547F	43.5					p.L547F	4.5		
							Loss			
							p.N645S	9.7		
PBRM1	p.R1359S	37.8					p.R1359S	5.3		
	p.G1324S	37.6								
							Loss			
							p.E620D	7.4		

Table 4. (Continued)

Gene	TS		TR1		TR2		TR3		TR4	
	AA Change	VAF	AA Change	VAF	AA Change	VAF	AA Change	VAF	AA Change	VAF
SETD2							Loss		Loss	
									p.P2363S	19.7
									p.T2354S	13.5
									p.A2349T	13.4
									p.A2293T	4.2
									p.P2216S	4.9
									p.P2160S	14.0
									p.Y2152F	11.5
									p.I1514V	17.2
									p.D1055E	9.5
									p.N1046S	8.9
									p.E1043A	9.3
									p.A526T	4.9
									p.N524H	5.0
									p.S511T	5.0
									p.Q7dup	9.7
									p.P6S	9.9
KEAP1							Loss		Loss	
							p.M147V	4.3	p.M147V	12.9
									p.P408S	8.4
									p.R380S	10.9
									p.S295A	7.8
									p.S293A	7.8
									p.M283T	7.4
									p.N251D	7.6
									p.V229A	8.8
									p.V197A	10.4
									p.V197M	10.1
									p.R135S	6.6

Table 4. (Continued)

Gene	TS		TR1		TR2		TR3		TR4	
	AA Change	VAF	AA Change	VAF	AA Change	VAF	AA Change	VAF	AA Change	VAF
SMARCA4	p.L196F	21.7					Loss			
	p.L396F	30.7					p.M342L	5.1		
ALK									Amplification	
									p.S1219T	4.4
									p.S1216N	4.7
									p.S1189A	4.1
									p.T901A	15.5
									p.Q897L	14.6
									p.N863S	6.4
									p.D854E	6.4
									p.I293M	4.1
									p.I293V	4.2
CRKL									p.A218T	23.9
									p.S220A	22.3
									p.G221S	21.8
									p.S222T	22.1
									p.S20T	9.6
									p.T228N	19.7
MYCN			Amplification							
			c.-251T>G	6.1						
			c.-237A>G	4.1						
			c.-209G>C	4.5						
			c.-204T>C	4.6						
			c.-199A>G	5.3						
			c.-198T>C	5.0						
			c.-196C>G	5.3						
			c.-186C>G	4.6						
			c.-181C>T	5.2						
SMARCB1			Loss							

Real time RT-PCR was performed using Glyceraldehyde-3-Phosphate Dehydrogenase (*GAPDH*) as housekeeping gene and the expression of *PTEN* and *CDH1* mRNA in TS and TR EMPD-PDX tumors were evaluated. The mRNA level of *PTEN* and *CDH1* in TR EMPD-PDX was found to be lower than that in TS EMPD-PDX (Figure 12).

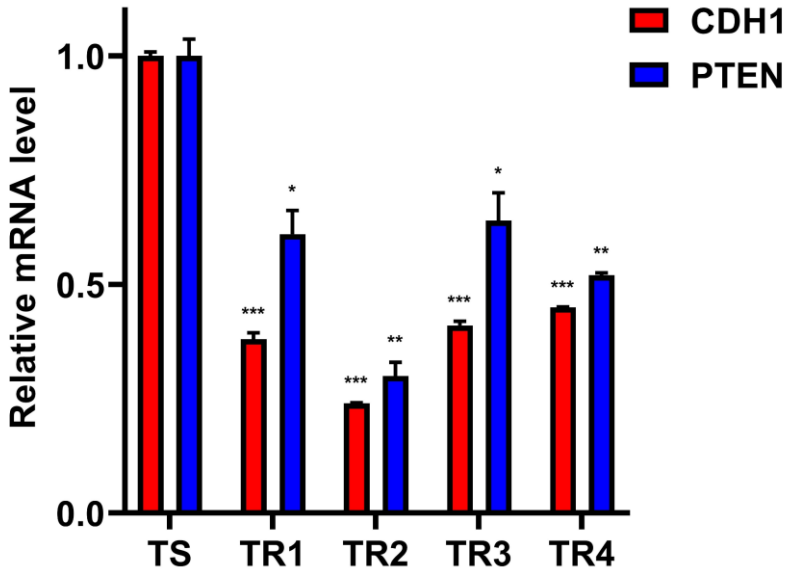

Figure 12. Comparison of mRNA expression levels of *PTEN* and *CDH1* between trastuzumab-sensitive (TS) and several trastuzumab-resistant (TR) EMPD tumors. In TR EMPD tumors, the expression of *PTEN* and *CDH1* was reduced at the mRNA level. Data are representative of duplicate experiments and are expressed as mean ± SD. *: $P < 0.05$, **: $P < 0.01$, ***: $P < 0.001$; compared to control TS tumor, by *t-test*.

TS and TR tumor tissues underwent histological examination with hematoxylin and eosin (H&E) staining as well as immunohistochemical (IHC) staining (Figure 13, A to H). TR tissues exhibited identical cell morphology (Figure 13, A and B), strong HER2 membrane localization (Figure 13, C and D), and either absent or weak E-cadherin staining (Figure 13, G and H), mirroring the characteristics observed in TS tissue. Protein expression of PTEN was present in TS but not TR tumors (Figure 13, E and F).

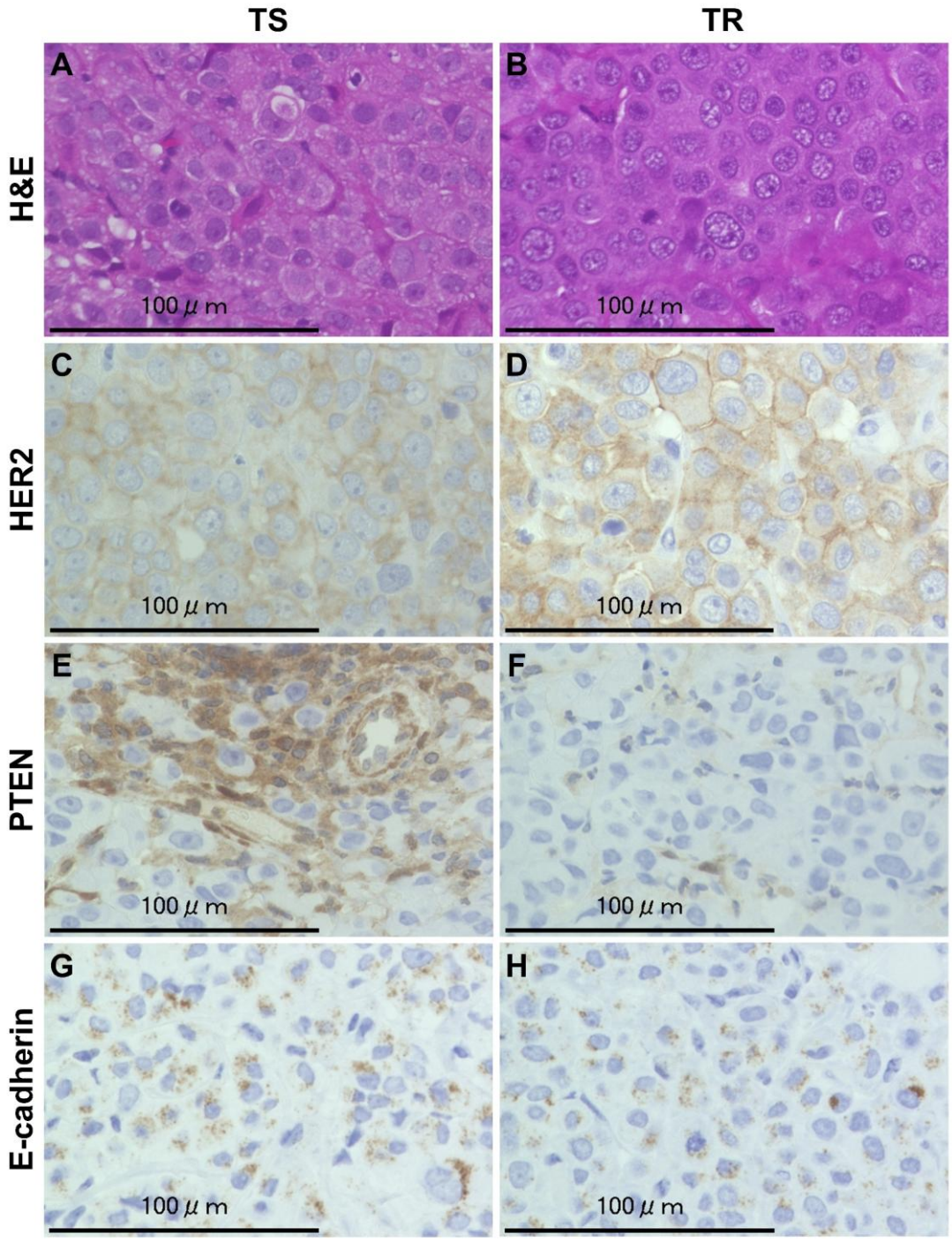

Figure 13. Histology of trastuzumab-sensitive (TS) and several trastuzumab-resistant (TR) EMPD-PDX tumors. Representative examples of H&E staining (A and B), immunohistochemical staining of HER2 (C and D), PTEN (E and F), and E-cadherin (G and H). Scale bars are 100 μm.

The loss of PTEN and E-cadherin proteins was confirmed by performing immunoblotting of cell lysates from TS and TR1 to TR4 tumors (Figure 14, A and B). Immunoblot analysis showed a notable reduction in PTEN protein expression levels in TR tumors compared to the control TS tumors. These results indicated that PTEN loss was induced after repeated trastuzumab treatment.

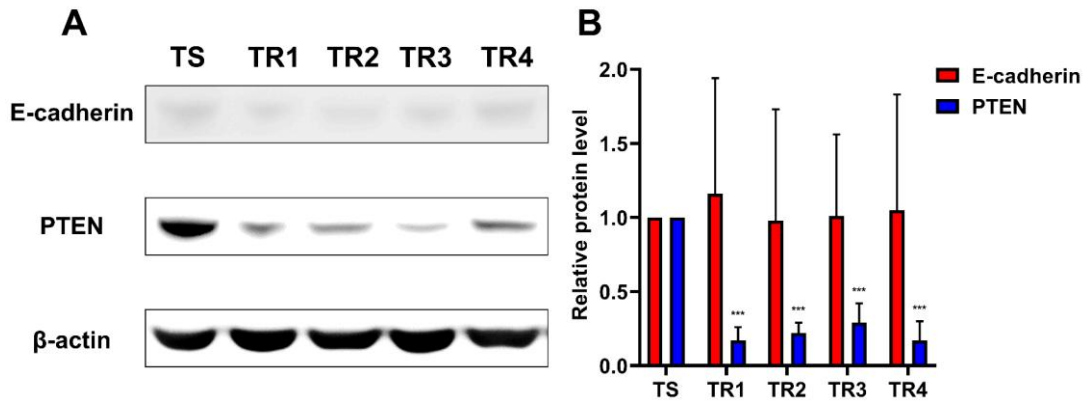

Figure 14. Immunoblot analysis of trastuzumab-sensitive (TS) and several trastuzumab-resistant (TR) EMPD-PDX tumors. Protein expression of E-cadherin and PTEN in TS and TR tumors. Immunoblot analysis showed that the expression levels of PTEN protein in TR tumors were significantly lower than in the control TS tumor. Data are representative of triplicate experiments and are expressed as mean ± SD. ***: $P < 0.001$; compared to control TS tumor, by *t-test*.

We identified a patient who had undergone trastuzumab treatment from Keio University. Biopsy samples were obtained from the 73-year-old Japanese male patient (Figure 15). After 7 months of trastuzumab plus docetaxel therapy, the combination therapy was becoming less and less effective. Additional samples were then taken from the perineum and a metastatic pelvic lymph node. We compared the immunohistochemical staining of PTEN and E-cadherin between skin samples (before and after chemotherapy) and a lymph node sample (after chemotherapy). Obvious alternations of the protein expression of E-cadherin and PTEN were not observed in these specimens. The results suggest that there are different causes of trastuzumab resistance other than PTEN loss. At the present time, the administration of trastuzumab against EMPD has not been covered by national insurance in Japan; thus, the number of such patients is very small. More clinical cases need to be collected for future investigation.

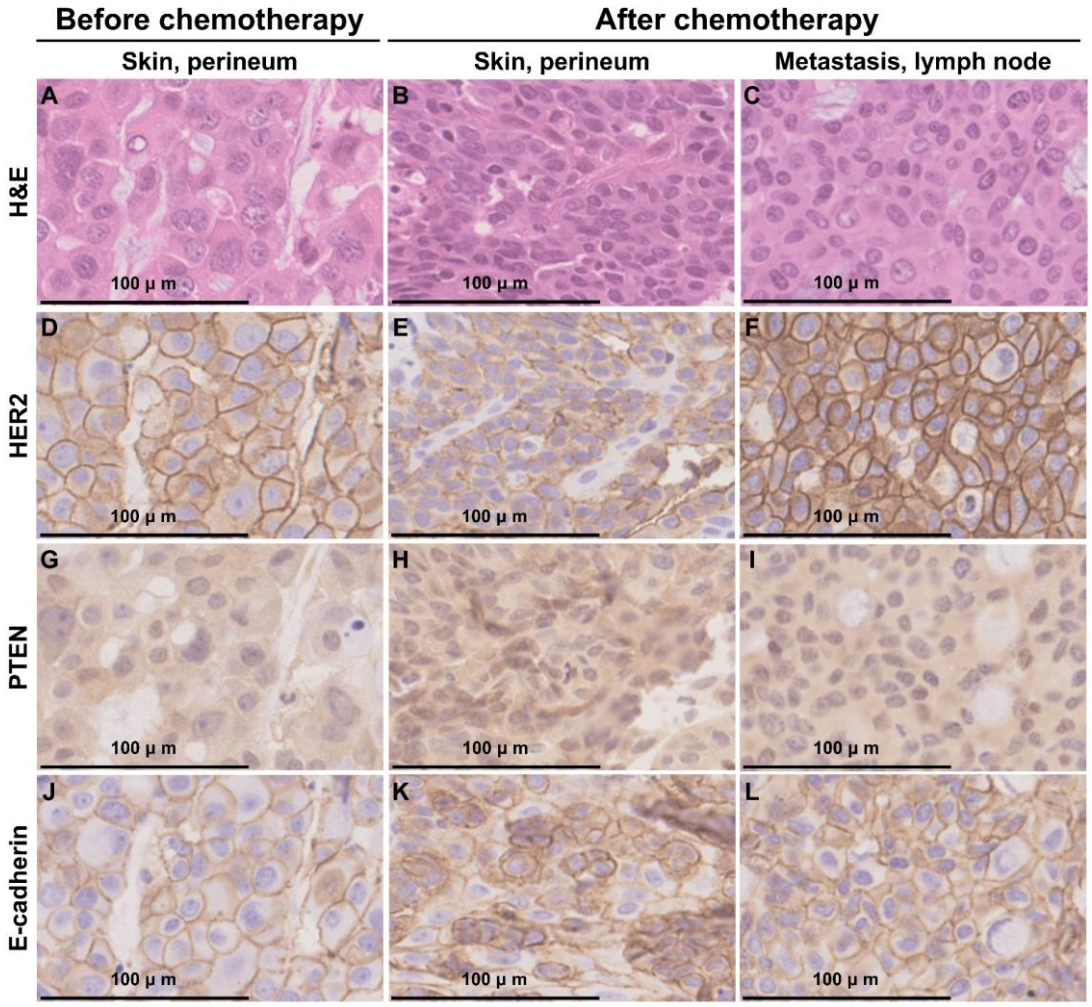

Figure 15. Histology and immunohistochemical analysis of a 73-year-old Japanese male EMPD patient before and after anti-HER2 chemotherapy. Representative examples of H&E staining (A to C), immunohistochemical staining of HER2 (D to F), PTEN (G to I), and E-cadherin (J to L). Biopsy samples were obtained from the perineum of a 73-year-old Japanese male patient. After 7 months of trastuzumab plus docetaxel therapy, additional biopsy samples were taken from the perineum and a metastatic pelvic lymph node. The left column shows specimens from the perineum before chemotherapy. The middle column indicates specimens from the perineum after chemotherapy. The right column shows specimens from a metastatic pelvic lymph node after chemotherapy (Scale bars = 100 μm).

The crucial function of *FOXA1* in EMPD was revealed in a study by Takeichi et al. While *FOXA1* mutation has been identified in 23% of EMPD patients (Takeichi et al. 2020; Mai et al. 2018; Sumitomo et al. 2023), the *FOXA1* gene was not included in our list of cancer gene sequencing (Table 1). To examine the expression of FOXA1 in TS and TR tumors, we performed immunohistochemical staining for FOXA1. In the results, FOXA1 was found to be strongly expressed in the nuclei of tumor cells in all of the examined TS and TR EMPD tumors (Figure 16 and Table 5). There were no obvious differences in FOXA1 expression between TS and TR tumors.

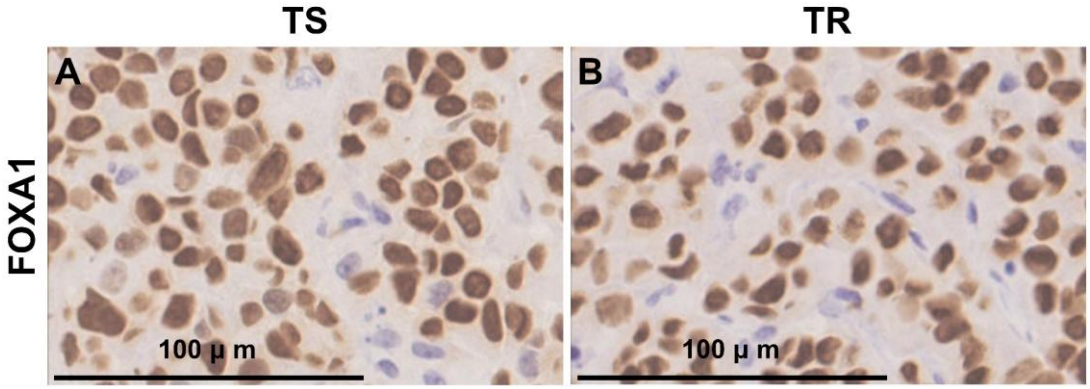

Figure 16. Immunohistochemical staining of FOXA1 in trastuzumab-sensitive (TS) and several trastuzumab-resistant (TR) EMPD-PDX tumors. Representative examples of immunohistochemical staining of FOXA1 (A and B). Scale bars are 100 μm.

Table 5. Comparison of FOXA1 expressing in trastuzumab-sensitive (TS) and several trastuzumab-resistant (TR) EMPD tumors

	FOXA1 staining	Allred score (Allred et al. 1998)
TS	+	8
TR1	+	7
TR2	+	8
TR3	+	7
TR4	+	8

***In vivo* effects of PTEN loss on signaling pathways of trastuzumab-resistant EMPD-PDX tumors**

We analysed five fresh lysate samples from EMPD tumors (one TS and four TR) to assess the expression of PTEN, Akt, phospho-Akt, extracellular signal-regulated kinase (ERK), phospho-ERK, p27 and β-actin through immunoblotting (Figure 17). PTEN expression in TR tumors was significantly lower than in TS tumors. Under normal PTEN conditions, TS tumors exhibited low phospho-Akt and phospho-ERK levels with a high p27 level. Conversely, several TR tumors showed significantly high phospho-Akt with low p27 levels. A notable inverse correlation between PTEN and phospho-Akt/p27 expression was observed.

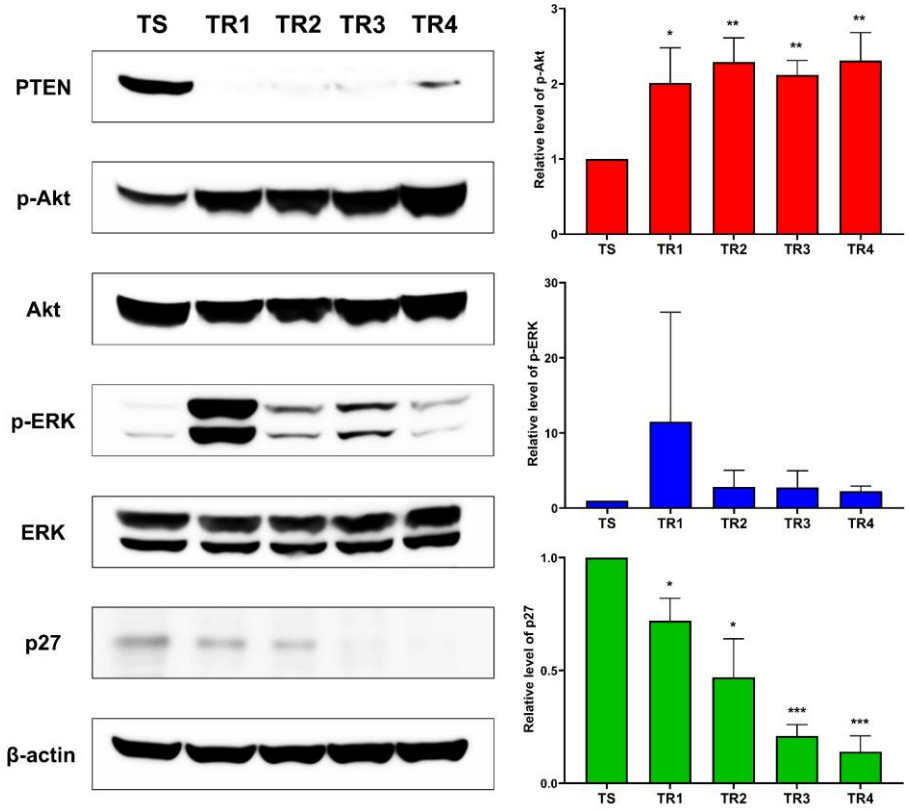

Figure 17. Trastuzumab-resistant (TR) EMPD-PDX tumors show loss of PTEN, increased Akt phosphorylation, and p27 downregulation. Immunoblotting for PTEN, phospho-Akt (p-Akt), Akt, phospho-ERK (p-ERK), ERK, p27 using tumor lysates from TS and TR1 to TR4 tumors. β-actin is shown as a loading control. The graph on the right demonstrates the densitometry analysis of the ratio of p-Akt/Akt, p-ERK/ERK, and p27/β-actin. Data are representative of triplicate experiments and are expressed as mean ± SD. *: $P < 0.05$, **: $P < 0.01$, ***: $P < 0.001$; compared to control TS tumor, by *t-test*.

PTEN inhibitors partially restored trastuzumab-mediated tumor regression

To investigate whether the loss of function of PTEN mediates the acquisition of trastuzumab resistance in TS EMPD tumor cells, we administered two PTEN inhibitors, BpV(HOpic) and SF1670, to TS EMPD-PDX models. Treatment with trastuzumab was found to suppress tumor progression, but treatment with BpV(HOpic) and SF1670 partially restored the inhibition of tumor growth mediated by the administration of trastuzumab (Figure 18).

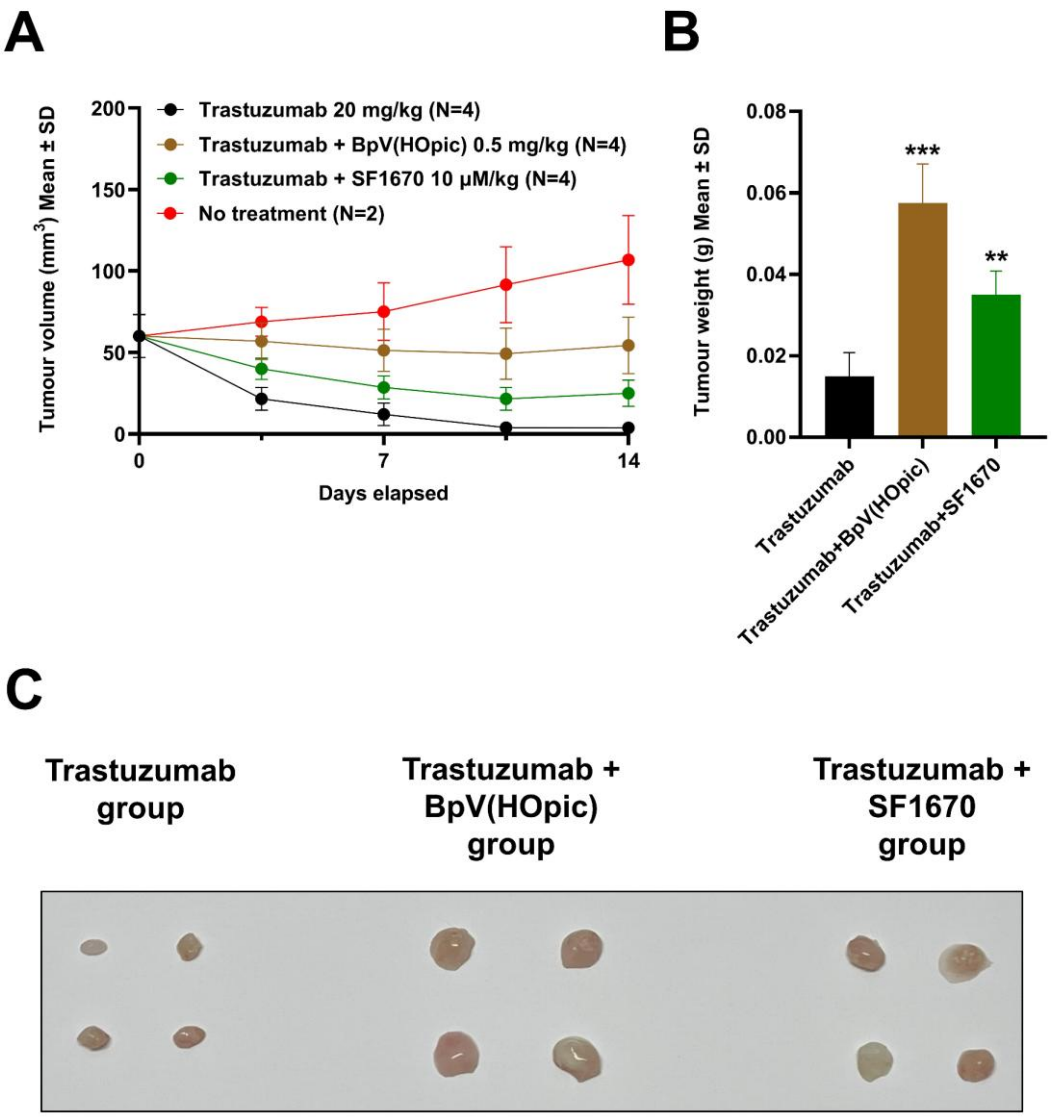

Figure 18. PTEN inhibitors partially restored trastuzumab-mediated tumor regression in the trastuzumab-sensitive EMPD-PDX mouse model. Tumor-bearing NOD/SCID mice were randomly assigned to a no-treatment group (red line), a trastuzumab group (black line), a BpV(HOpic) group (brown line), or a SF1670 group

(green line). The no-treatment group (n = 2) was administered with intraperitoneal injection of PBS 100 μL every day for 14 days. The trastuzumab group (n = 4) received intraperitoneal injections of trastuzumab (10 mg/kg) twice per week for 14 days. In the BpV(HOpic) group (n = 4, 0.5 mg/kg), mice were intraperitoneally pretreated with BpV(HOpic) for 3 days, followed by trastuzumab (10 mg/kg) twice per week and BpV(HOpic) every day for 14 days. In the SF1670 group (n = 4, 10 μM/kg), mice were intraperitoneally pretreated with SF1670 for 3 days, followed by trastuzumab (10 mg/kg) twice per week and SF1670 every day for 14 days. Tumor volumes were measured twice per week (A). The tumors were extracted, and their weights were measured 14 days after treatment initiation (B and C). The results are shown as mean ± SD. **: $P < 0.01$, ***: $P < 0.001$; compared to trastuzumab group, by *t-test*.

Treatment experiments using the trastuzumab-resistant EMPD-PDX mouse model

This article presents the first reported preclinical animal model for TR EMPD, a rarity possibly attributed to challenges in obtaining EMPD-PDX tissues (Maeda et al. 2020). To investigate the effects of targeted therapy and chemotherapy on TR EMPD-PDX, we conducted treatment experiments that mimicked clinical scenarios (Yoshino et al. 2016; Kato et al. 2019; Karam et al. 2008). Considering the loss of PTEN in TR EMPD-PDX, we administered HER2-targeted therapies, including trastuzumab and lapatinib (Figure 19). Lapatinib caused a marked inhibition of tumor growth, while no significant difference was noted between the control and trastuzumab groups.

Due to the loss of PTEN in TR EMPD-PDX, we administered HER2-targeted therapies, including abemaciclib and palbociclib (Figure 20) (Kitamura et al. 2022). Both abemaciclib and palbociclib significantly inhibited tumor growth compared to the control groups.

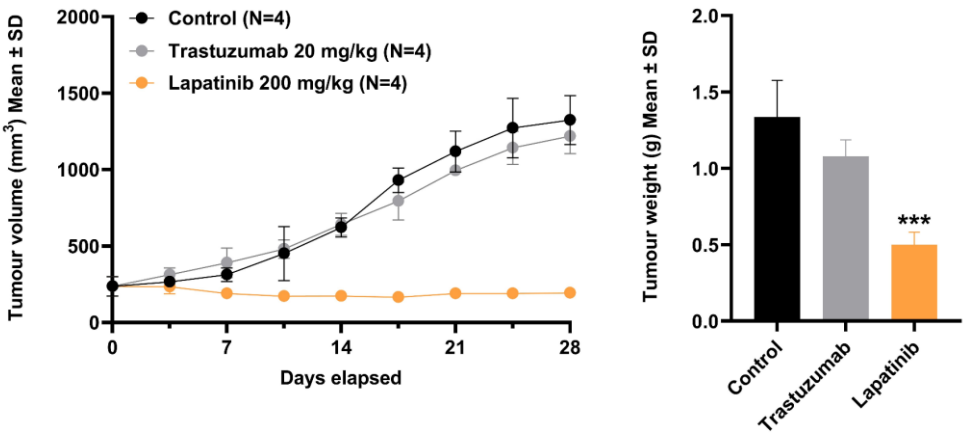

Figure 19. HER2-targeted therapies suppress tumor growth in the trastuzumab-resistant EMPD-PDX mouse model. Tumor-bearing NOD/SCID mice were randomly assigned to a control group (black line), a trastuzumab group (grey line), or a lapatinib group (orange line). Trastuzumab (n = 4, 20 mg/kg) was administered intraperitoneally once per week. Lapatinib (n = 4, 200 mg/kg) was administered orally once per day. Tumor volumes were measured twice per week. The tumors were extracted, and their weights were measured 28 days after treatment initiation. The results are shown as mean ± SD. ***: $P < 0.001$; compared to control group, by *t-test*.

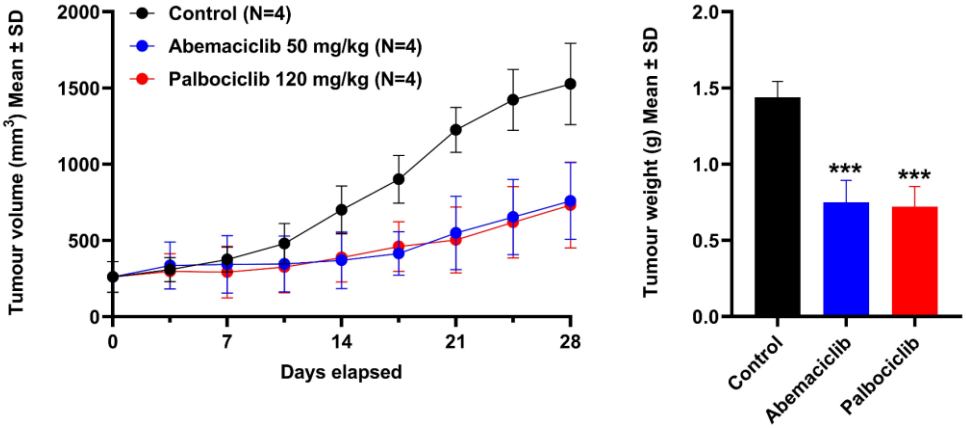

Figure 20. Cyclin-dependent kinase 4/6 inhibitors suppress tumor growth in the trastuzumab-resistant EMPD-PDX mouse model. Tumor-bearing NOD/SCID mice were randomly assigned to a control group (black line), an abemaciclib group (blue line), or a palbociclib group (red line). Abemaciclib (n = 4, 50 mg/kg) was administered orally once daily. Palbociclib (n = 4, 120 mg/kg) was administered orally once daily. Tumor volumes were measured twice per week. The tumors were extracted, and their weights were measured 28 days after treatment initiation. The results are shown as mean ± SD. ***: $P < 0.001$; compared to control group, by *t-test*.

In terms of cytotoxic chemotherapy, our xenograft model demonstrated positive responses to eribulin, docetaxel, and trastuzumab deruxtecan (T-DXd), which are known for their efficacy in metastatic EMPD and EMPD-PDX models (Tokuchi et al. 2022). We specifically tested eribulin and T-DXd monotherapy, established as effective second-line treatments for breast cancer (Swain, Shastry, and Hamilton 2023; Fleeman et al. 2019). Eribulin therapies (1.5 mg/kg/week) and a single dose of T-DXd (10 mg/kg) completely eradicated TR EMPD-PDX, with no observed relapse for 14 days (Figure 21).

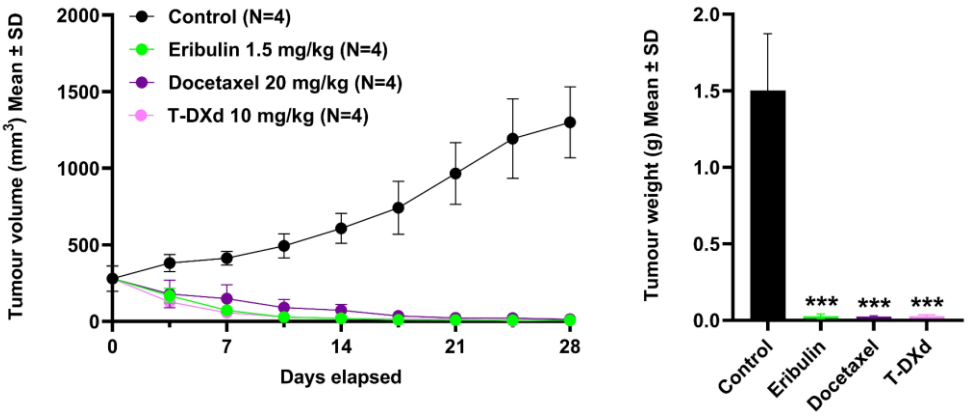

Figure 21. Cytotoxic agents suppress tumor growth in the trastuzumab-resistant EMPD-PDX mouse model. Tumor-bearing NOD/SCID mice were randomly assigned to a control group (black line), an eribulin group (green line), a docetaxel group (purple line), or a T-DXd group (pink line). Eribulin (n = 4, 1.5 mg/kg) was administered intravenously once weekly. Docetaxel group (n = 4, 20 mg/kg) was administered intraperitoneally once per week. T-DXd (n = 4, 10 mg/kg) was administered intravenously as a single dose. Tumor volumes were measured twice per week. The tumors were extracted, and their weights were measured 28 days after treatment initiation. The results are shown as mean ± SD. ***: $P < 0.001$; compared to control group, by *t-test*.

Discussion

The current research introduced a TR EMPD-PDX model that displayed a morphological resemblance to the naïve tumors, as well as a similar level of HER2 expression. It showed a distinctive loss of PTEN expression, suggesting a potential cause of trastuzumab resistance. In addition, we highlighted promising therapeutic approaches involving HER2-targeted therapies and other types of cytotoxic chemotherapy.

In certain cases of EMPD, HER2 overexpression, detected via immunohistochemistry and in situ hybridization, is found to coincide with *ERBB2* mutations (Tanaka et al. 2013; Kiniwa et al. 2019). Some clinical studies have indicated responsiveness to anti-HER2 agents in invasive EMPD patients (Vornicova et al. 2014). However, repeated trastuzumab treatments may induce acquired resistance (Nordmann et al. 2019). Our study, employing the TR EMPD-PDX model, confirmed the presence of a mutation in PTEN. Notably, this PTEN mutation is found in ~80% of patients with Cowden syndrome, a cancer predisposition syndrome inherited through germline mutations of *PTEN* (Gustafson et al. 2007). This syndrome increases individuals' susceptibility to hamartomas and the risk of developing malignancies (Gammon, Jasperson, and Champine 2016).

PTEN serves as a crucial negative regulator within the PI3K/Akt/mTOR signaling pathway, which plays a pivotal role in governing fundamental cellular processes, including proliferation, growth, survival, and metabolism (Figure 22) (Fruman and Rommel 2014). Deregulation of the PI3K/AKT/mTOR axis is common in cancers, with frequent mutations affecting major signaling components (Álvarez-Garcia et al. 2019). Loss of PTEN disrupts the regulation of PIP3 levels, promoting hyper-activation of the Akt/mTOR pathway and ultimately leading to cellular transformation and carcinogenesis. EMPD, resembling Paget's breast cancer, often shows overexpression of HER2 or hormone receptors (HRs) (Angelico et al. 2020). Numerous studies support the common observation of PTEN loss in breast cancer, and PTEN-deficient cases exhibit poorer responses to trastuzumab-based therapy (Nagata et al. 2004).

Due to the limited availability of advanced EMPD cases, we generated four TR EMPD-PDX strains from a single naïve EMPD-PDX in our study. Intriguingly, these TR EMPD-PDX consistently exhibited a loss-of-function mutation in the PTEN gene. This supports the significance of this mutation in the development of trastuzumab resistance, not only in breast cancer but also in EMPD. Previous studies have indicated that PTEN loss activates both the PI3K/Akt and MAPK signaling pathways in HER2/neu breast carcinoma. Restoring PTEN function effectively suppresses both PI3K and MAPK

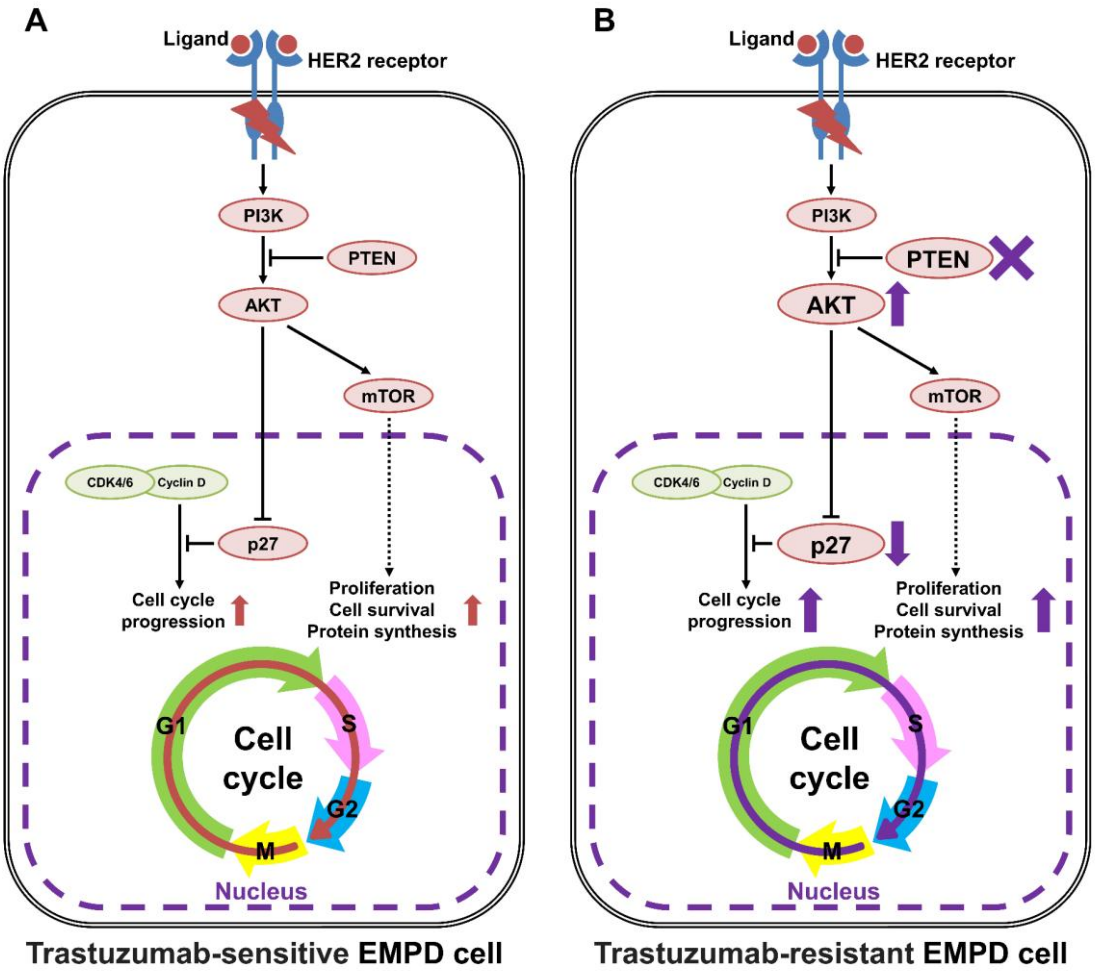

Figure 22. Schematic illustration of the pathogenic mechanisms involved in trastuzumab-resistant EMPD-PDX. (A) In TS EMPD cells, activation of the HER2 signaling pathway results in vigorous tumor cell proliferation, which can be blocked by trastuzumab. (B) Loss of PTEN contributes to high Akt activation and down-regulation of p27, and induces cell cycle progression and proliferation of TR EMPD cells. A multitude of targets exists within signaling pathways that can be harnessed as focal points for various therapeutic agents.

signaling, leading to significant tumor regression (Ebbesen et al. 2016). This finding may help to clarify the ambiguous ERK phosphorylation observed in our results (Figure 17). Another crucial aspect of trastuzumab resistance is p27Kip1 (p27). The cyclin-dependent kinase inhibitor p27Kip1 is diminished in TR cells, and supplementing p27Kip1 externally enhances trastuzumab sensitivity in breast cancer cells (Nahta et al. 2004).

In the context of EMPD, Nordmann et al. reported a case of EMPD with secondary anti-HER2 treatment resistance (Nordmann et al. 2019). Genomic analysis revealed additional alterations, including *ERBB3* A232V and *PIK3CA* G106V point mutations, as well as *MET* and *CDK6* amplification, suggesting a potential cause of resistance to treatment. The *PIK3CA* G106V mutation, which activates the catalytic subunit of phosphoinositide 3-kinase, stimulates lipid kinase activity and is associated with resistance to trastuzumab (Shi et al. 2019). In addition, genomic analysis of clinical samples from EMPD revealed recurrent mutations in genes, predominantly *PIK3CA* (Takeichi et al. 2020; Kiniwa et al. 2019; Barth et al. 2015) and occasionally *PTEN* (Barth et al. 2015; Zhang et al. 2019). This finding aligns with our experimental results, indicating that the PI3K/AKT/mTOR pathway contributes to pathogenesis and trastuzumab resistance in EMPD.

In this study, both TS and TR tumors showed very low expression levels of E-cadherin, the protein product of the *CDH1* gene. We observed no significant difference in E-cadherin levels between TS and TR tumors (Figure 14, A and B). To explore the mechanism of trastuzumab resistance in clinical samples, we selected a patient who had received trastuzumab treatment. Biopsy samples were obtained from a 73-year-old Japanese male patient (Figure 15). No significant changes were detected in the protein expression levels of E-cadherin in the samples. These results suggest that E-cadherin might not be involved in trastuzumab resistance. Previous studies have not reported any associations between the loss of E-cadherin and resistance to trastuzumab. On the other hand, loss of PTEN could be linked to trastuzumab resistance in HER2-positive breast cancer cells and patients (Nagata et al. 2004; Gallardo et al. 2012; Y. Wang et al. 2013). In our EMPD-PDX models, TR tumors showed a significant decrease in PTEN protein expression compared to TS tumors (Figure 14, A and B) (Kim et al. 2017; Pohlmann, Mayer, and Mernaugh 2009). Consequently, we focused our efforts on investigating trastuzumab resistance associated with PTEN.

This study demonstrated the antitumor effects of both targeted and cytotoxic therapy. With respect to targeted therapy, we administered lapatinib (Figure 19) (Maeda et al. 2020), abemaciclib, and palbociclib (Figure 20) (Kitamura et al. 2022) in TR EPMD-PDX models. Lapatinib, a reversible dual kinase inhibitor targeting EGFR and HER2

(Rusnak et al. 2001), proved effective in clinical trials for breast cancer patients with low PTEN tumors (Dave et al. 2011). Abemaciclib and palbociclib, which are CDK4/6 inhibitors, partially suppressed tumor growth in TR EMPD-PDX compared to naïve EMPD-PDX (Kitamura et al. 2022). The present study revealed that docetaxel and eribulin exhibited high efficacy against TR EMPD-PDX xenografts (Figure 21), suggesting these agents as potential treatment options. Docetaxel, a semi-synthetic taxane, induces the polymerisation of tubulin monomers and inhibits depolymerisation, leading to mitotic cell arrest, and causing cell death (Imran et al. 2020). Docetaxel is the preferred firstline-chemotherapy regimen when combined with trastuzumab plus pertuzumab for HER2-positive metastatic breast cancer (Swain et al. 2020). In addition, it serves as the first-line chemotherapy for metastatic EMPD (Yoshino et al. 2016; Hatta et al. 2024). Eribulin, an inhibitor of microtubule dynamics, exerts its effects via a tubulin-based antimitotic mechanism, leading to G2/M cell-cycle blockage, disruption of mitotic spindles, and apoptotic cell death. Eribulin has demonstrated efficacy against taxane refractory metastatic breast cancer (Fernández-Laguna et al. 2023), and it has shown effectiveness when combined with trastuzumab in pretreated HER2-positive breast cancer (Lutrino et al. 2020). Also, our previous study suggests the promising potential of eribulin against EMPD-PDX models (Maeda et al. 2020). The present study confirms the positive impact of both docetaxel and eribulin, regardless of trastuzumab resistance.

Trastuzumab deruxtecan (T-DXd) is another highly effective drug for TR EMPD-PDX tumors (Figure 21). T-DXd is an antibody-drug conjugate (ADC) that combines trastuzumab with a cytotoxic agent, an exatecan derivative, acting as a topoisomerase I inhibitor (Nakada et al. 2016). T-DXd broadens therapeutic options and enhances efficacy against HER2-positive TR breast cancer (Z.H. Wang et al. 2022; Wu et al. 2022). The promising effectiveness of T-DXd against EMPD-PDX models arises from its mechanism, which involves the recognition and binding of the monoclonal antibody backbone to the extracellular domain of HER2 (Figure 23) (Najjar et al. 2022). This is followed by internalization of the ADC-antigen complex via HER2-mediated endocytosis and subsequent intracellular release of the cytotoxic cargo (Thomas, Teicher, and Hassan 2016), inducing cell death independent of trastuzumab resistance. Our TR EMPD-PDX exhibited strong HER2 staining (Figure 13D), indicating that T-DXd could be internalised via HER2-mediated endocytosis.

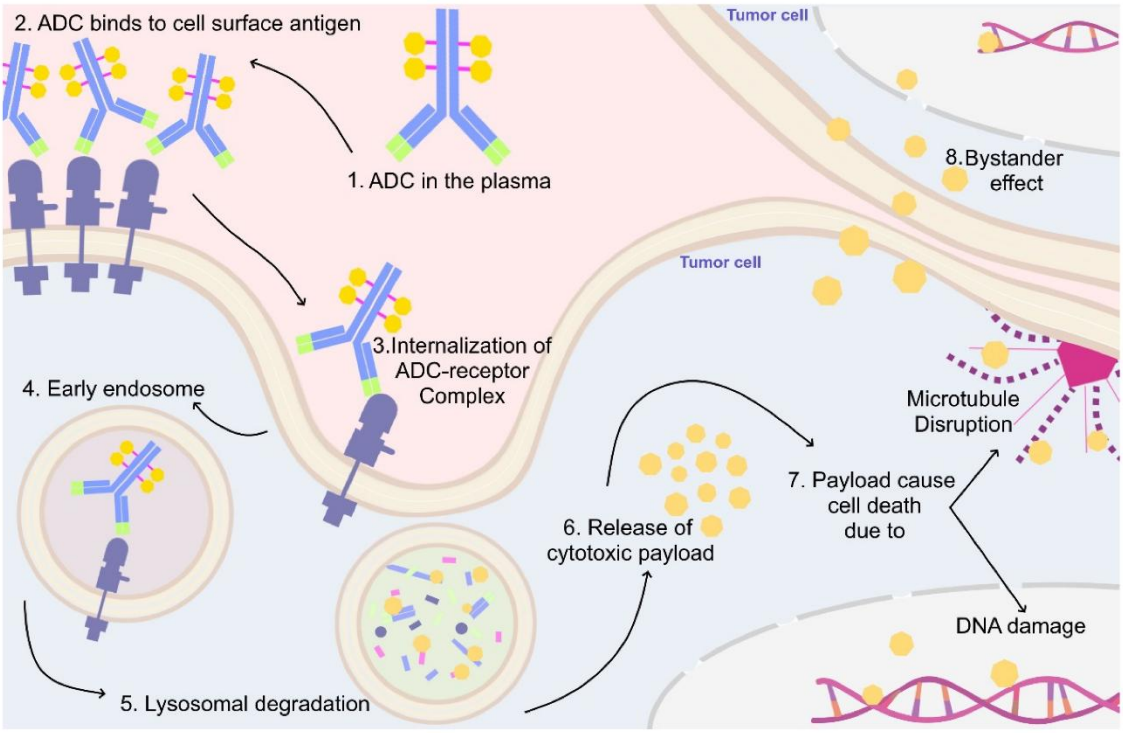

Figure 23. Antibody-drug conjugate mechanism of action (Najjar et al. 2022). Following ADC administration, (1) it enters the bloodstream, where (2) the antibody component binds to the overexpressed target antigen or receptor on tumor cells (e.g., HER2). (3) Upon binding, the ADC-receptor complex undergoes receptor-mediated endocytosis, leading to endosome formation (4). Within the lysosome, (5) the complex is degraded, cleaving the linker and releasing the cytotoxic payloads (6). Depending on the payload type, (7) it induces cell death either by DNA damage or microtubule disruption. Furthermore, (8) membrane-permeable payloads can exert cytotoxic effects on neighboring cells through the bystander effect, independent of their antigen expression.

Conclusion

- TR EMPD-PDX mouse models were established by serially propagating *ERBB2* S310F-mutated tumors with trastuzumab dose escalation, categorizing growth rates across multiple generations.
- TR EMPD-PDX tumors exhibited deficiencies in *PTEN* and *CDH1* genes, along with reduced mRNA and protein levels of PTEN compared to TS tumors.
- Based on the limited clinical case, immunohistochemical analysis revealed no significant changes in PTEN and E-cadherin expression, suggesting trastuzumab resistance may arise from mechanisms other than PTEN loss.
- FOXA1 was strongly expressed in all TS and TR EMPD tumors, with no significant differences noted between the two groups.
- PTEN loss in TR EMPD-PDX tumors led to increased phospho-Akt levels and decreased p27, indicating altered signaling pathways.
- PTEN inhibitors BpV(HOpic) and SF1670 partially restored trastuzumab-mediated tumor regression in TS EMPD-PDX models.
- Treatment experiments using the TR EMPD-PDX mouse model showed significant tumor growth inhibition with lapatinib, abemaciclib, palbociclib, eribulin, docetaxel, and T-DXd.

This study successfully establishes a TR EMPD-PDX model, highlighting the critical role of PTEN loss in driving resistance mechanisms. The model mirrors the characteristics of naïve tumors, particularly in terms of HER2 expression and the presence of *ERBB2* S310F mutation. Through comprehensive genomic and protein expression analyses, we demonstrate that trastuzumab resistance in EMPD is not solely a consequence of HER2 overexpression but is intricately linked to specific genetic alterations, including the loss of *PTEN*. Moreover, our exploration of various therapeutic strategies reveals promising avenues for treatment, showcasing the efficacy of HER2-targeted therapies like lapatinib and CDK inhibitors, as well as cytotoxic agents such as eribulin, docetaxel, and T-DXd in suppressing tumor growth.

To further advance research in this area, it is crucial to investigate additional genetic and epigenetic factors contributing to trastuzumab resistance beyond *PTEN* loss. Expanding the current study to include larger patient cohorts will enhance our understanding of the molecular pathways involved and help validate the findings from our preclinical model. Additionally, exploring combination therapies that target multiple pathways simultaneously could improve treatment efficacy and outcomes for patients

with advanced EMPD. Ultimately, these efforts will contribute to the development of innovative therapeutic strategies aimed at overcoming resistance and enhancing patient care in this challenging disease context.

Acknowledgement

I would like to express my deepest gratitude to Professor Hideyuki Ujiie of the Department of Dermatology, Faculty of Medicine and Graduate School of Medicine, Hokkaido University, and Professor Kenzo Takahashi of the Department of Dermatology, Graduate School of Medicine, University of the Ryukyus, for providing me with the opportunity to conduct this research and for their invaluable guidance and support. I am also sincerely grateful to Dr. Teruki Yanagi for his direct supervision. Furthermore, I would like to extend my heartfelt thanks to all the authors who contributed to this study. Lastly, I would like to express my sincere appreciation to the faculty members, technicians, and administrative staff of the Department of Dermatology, Faculty of Medicine and Graduate School of Medicine, Hokkaido University, as well as the Graduate School of Medicine, University of the Ryukyus.

This work was supported by Hokkaido University DX (EXEX) Doctoral Fellowship

Conflict of interest

The authors have no conflicts of interest to declare.

Reference

Allred, D. C., J. M. Harvey, M. Berardo, and G. M. Clark. 1998. "Prognostic and predictive factors in breast cancer by immunohistochemical analysis." *Mod Pathol* 11 (2): 155-68.

Álvarez-Garcia, V., Y. Tawil, H. M. Wise, and N. R. Leslie. 2019. "Mechanisms of PTEN loss in cancer: It's all about diversity." *Semin Cancer Biol* 59: 66-79. https://doi.org/10.1016/j.semcancer.2019.02.001.

Angelico, G., A. Santoro, F. Inzani, P. Straccia, D. Arciuolo, A. Mulè, M. Valente, S. Spadola, N. D'Alessandris, G. Garganese, F. Cianfrini, A. Piermattei, G. Scambia, and G. F. Zannoni. 2020. "Hormonal Environment and HER2 Status in Extra-Mammary Paget's Disease (eMPD): A Systematic Literature Review and Meta-Analysis with Clinical Considerations." *Diagnostics (Basel)* 10 (12). https://doi.org/10.3390/diagnostics10121040.

Barth, P., E. Dulaimi Al-Saleem, K. W. Edwards, S. Z. Millis, Y. N. Wong, and D. M. Geynisman. 2015. "Metastatic Extramammary Paget's Disease of Scrotum Responds Completely to Single Agent Trastuzumab in a Hemodialysis Patient: Case Report, Molecular Profiling and Brief Review of the Literature." *Case Rep Oncol Med* 2015: 895151. https://doi.org/10.1155/2015/895151.

Cho, H. S., K. Mason, K. X. Ramyar, A. M. Stanley, S. B. Gabelli, D. W. Denney, Jr., and D. J. Leahy. 2003. "Structure of the extracellular region of HER2 alone and in complex with the Herceptin Fab." *Nature* 421 (6924): 756-60. https://doi.org/10.1038/nature01392.

Cohen, J. M., S. R. Granter, and A. E. Werchniak. 2015. "Risk stratification in extramammary Paget disease." *Clin Exp Dermatol* 40 (5): 473-8. https://doi.org/10.1111/ced.12690.

Dave, B., I. Migliaccio, M. C. Gutierrez, M. F. Wu, G. C. Chamness, H. Wong, A. Narasanna, A. Chakrabarty, S. G. Hilsenbeck, J. Huang, M. Rimawi, R. Schiff, C. Arteaga, C. K. Osborne, and J. C. Chang. 2011. "Loss of phosphatase and tensin homolog or phosphoinositol-3 kinase activation and response to trastuzumab or lapatinib in human epidermal growth factor receptor 2-overexpressing locally advanced breast cancers." *J Clin Oncol* 29 (2): 166-73. https://doi.org/10.1200/jco.2009.27.7814.

Ebbesen, S. H., M. Scaltriti, C. U. Bialucha, N. Morse, E. R. Kastenhuber, H. Y. Wen, L. E. Dow, J. Baselga, and S. W. Lowe. 2016. "Pten loss promotes MAPK pathway dependency in HER2/neu breast carcinomas." *Proc Natl Acad Sci U S A* 113

(11): 3030-5. https://doi.org/10.1073/pnas.1523693113.

Feng, Q., X. Li, X. Qin, C. Yu, Y. Jin, and X. Qian. 2020. "PTEN inhibitor improves vascular remodeling and cardiac function after myocardial infarction through PI3k/Akt/VEGF signaling pathway." *Mol Med* 26 (1): 111. https://doi.org/10.1186/s10020-020-00241-8.

Fernández-Laguna, C. L., I. Maray, L. Macia-Rivas, C. Álvarez-Asteinza, S. Fernández-Lastras, V. Velasco Durántez, M. Carbajales Álvarez, and A. Lozano-Blázquez. 2023. "Eribulin in metastatic breast cancer: Real world data." *Breast Dis* 42 (1): 349-360. https://doi.org/10.3233/bd-230031.

Fleeman, N., A. Bagust, R. Duarte, M. Richardson, S. Nevitt, A. Boland, E. Kotas, J. McEntee, and N. Thorp. 2019. "Eribulin for Treating Locally Advanced or Metastatic Breast Cancer After One Chemotherapy Regimen: An Evidence Review Group Perspective of a NICE Single Technology Appraisal." *Pharmacoecon Open* 3 (3): 293-302. https://doi.org/10.1007/s41669-018-0114-z.

Fruman, D. A., and C. Rommel. 2014. "PI3K and cancer: lessons, challenges and opportunities." *Nat Rev Drug Discov* 13 (2): 140-56. https://doi.org/10.1038/nrd4204.

Fry, D. W., P. J. Harvey, P. R. Keller, W. L. Elliott, M. Meade, E. Trachet, M. Albassam, X. Zheng, W. R. Leopold, N. K. Pryer, and P. L. Toogood. 2004. "Specific inhibition of cyclin-dependent kinase 4/6 by PD 0332991 and associated antitumor activity in human tumor xenografts." *Mol Cancer Ther* 3 (11): 1427-38.

Fukuda, K., and T. Funakoshi. 2018. "Metastatic Extramammary Paget's Disease: Pathogenesis and Novel Therapeutic Approach." *Front Oncol* 8: 38. https://doi.org/10.3389/fonc.2018.00038.

Gallardo, A., E. Lerma, D. Escuin, A. Tibau, J. Muñoz, B. Ojeda, A. Barnadas, E. Adrover, L. Sánchez-Tejada, D. Giner, F. Ortiz-Martínez, and G. Peiró. 2012. "Increased signalling of EGFR and IGF1R, and deregulation of PTEN/PI3K/Akt pathway are related with trastuzumab resistance in HER2 breast carcinomas." *Br J Cancer* 106 (8): 1367-73. https://doi.org/10.1038/bjc.2012.85.

Gammon, A., K. Jasperson, and M. Champine. 2016. "Genetic basis of Cowden syndrome and its implications for clinical practice and risk management." *Appl Clin Genet* 9: 83-92. https://doi.org/10.2147/tacg.S41947.

Ghazawi, F. M., N. Iga, R. Tanaka, Y. Fujisawa, K. Yoshino, C. Yamashita, Y. Yamamoto, T. Fujimura, T. Yanagi, H. Hata, S. Matsushita, M. Le, S. F. Roy, F.

Lagacé, Y. Ishida, K. Kabashima, and A. Otsuka. 2021. "Demographic and clinical characteristics of extramammary Paget's disease patients in Japan from 2000 to 2019." *J Eur Acad Dermatol Venereol* 35 (2): e133-e135. https://doi.org/10.1111/jdv.16868.

Giordano, S. H., M. A. B. Franzoi, S. Temin, C. K. Anders, S. Chandarlapaty, J. R. Crews, J. J. Kirshner, I. E. Krop, N. U. Lin, A. Morikawa, D. A. Patt, J. Perlmutter, N. Ramakrishna, and N. E. Davidson. 2022. "Systemic Therapy for Advanced Human Epidermal Growth Factor Receptor 2-Positive Breast Cancer: ASCO Guideline Update." *J Clin Oncol* 40 (23): 2612-2635. https://doi.org/10.1200/jco.22.00519.

Gustafson, S., K. M. Zbuk, C. Scacheri, and C. Eng. 2007. "Cowden syndrome." *Semin Oncol* 34 (5): 428-34. https://doi.org/10.1053/j.seminoncol.2007.07.009.

Hatta, N., D. Ogata, J. Asai, T. Maekawa, T. Ito, T. Takenouchi, Y. Kiniwa, A. Miyashita, T. Miyagawa, I. Muto, Y. Yamamoto, T. Nagano, Y. Kiyohara, E. Nakano, S. Ohe, B. Yamaguchi, M. Fukuyama, T. Matsuya, A. Tsutsumida, K. Namikawa, and N. Yamazaki. 2024. "Recent treatment and prognosis in 643 patients with extramammary Paget's disease." *Exp Dermatol* 33 (2): e15030. https://doi.org/10.1111/exd.15030.

Imran, Mohammad, Sadaf Saleem, Aiswarya Chaudhuri, Javed Ali, and Sanjula Baboota. 2020. "Docetaxel: An update on its molecular mechanisms, therapeutic trajectory and nanotechnology in the treatment of breast, lung and prostate cancer." *Journal of Drug Delivery Science and Technology* 60: 101959.

Irie, H., R. Kawabata, Y. Fujioka, F. Nakagawa, H. Itadani, H. Nagase, K. Ito, J. Uchida, S. Ohkubo, and K. Matsuo. 2020. "Acquired resistance to trastuzumab/pertuzumab or to T-DM1 in vivo can be overcome by HER2 kinase inhibition with TAS0728." *Cancer Sci* 111 (6): 2123-2131. https://doi.org/10.1111/cas.14407.

Ishizuki, S., and Y. Nakamura. 2021. "Extramammary Paget's Disease: Diagnosis, Pathogenesis, and Treatment with Focus on Recent Developments." *Curr Oncol* 28 (4): 2969-2986. https://doi.org/10.3390/curroncol28040260.

Karam, A., J. S. Berek, A. Stenson, J. Rao, and O. Dorigo. 2008. "HER-2/neu targeting for recurrent vulvar Paget's disease A case report and literature review." *Gynecol Oncol* 111 (3): 568-71. https://doi.org/10.1016/j.ygyno.2007.12.014.

Kato, M., K. Yoshino, T. Maeda, K. Nagai, S. Oaku, A. Hiura, and Y. Fujisawa. 2019. "Single-agent taxane is useful in palliative chemotherapy for advanced extramammary Paget disease: a case series." *Br J Dermatol* 181 (4): 831-832.

https://doi.org/10.1111/bjd.17922.

Kim, C., C. K. Lee, H. J. Chon, J. H. Kim, H. S. Park, S. J. Heo, H. J. Kim, T. S. Kim, W. S. Kwon, H. C. Chung, and S. Y. Rha. 2017. "PTEN loss and level of HER2 amplification is associated with trastuzumab resistance and prognosis in HER2-positive gastric cancer." *Oncotarget* 8 (69): 113494-113501. https://doi.org/10.18632/oncotarget.23054.

Kiniwa, Y., J. Yasuda, S. Saito, R. Saito, I. N. Motoike, I. Danjoh, K. Kinoshita, N. Fuse, M. Yamamoto, and R. Okuyama. 2019. "Identification of genetic alterations in extramammary Paget disease using whole exome analysis." *J Dermatol Sci* 94 (1): 229-235. https://doi.org/10.1016/j.jdermsci.2019.03.006.

Kitamura, S., T. Yanagi, T. Maeda, and H. Ujiie. 2022. "Cyclin-dependent kinase 4/6 inhibitors suppress tumor growth in extramammary Paget's disease." *Cancer Sci* 113 (2): 802-807. https://doi.org/10.1111/cas.15234.

Lutrino, E. S., L. Orlando, A. Febbraro, M. Giampaglia, C. Zamagni, P. Schiavone, C. Scavelli, G. Dima, P. Fedele, G. Giordano, D. Bilancia, A. M. Quaranta, D. Rubino, G. Filippelli, C. Fontanella, C. Caliolo, A. Marino, N. Calvani, P. Ferrara, and S. Cinieri. 2020. "Eribulin plus trastuzumab in pretreated HER2-positive advanced breast cancer patients: safety and efficacy. An Italian experience." *Tumori* 106 (4): 301-305. https://doi.org/10.1177/0300891619887225.

Maeda, T., S. Kitamura, H. Nishihara, and T. Yanagi. 2020. "Extramammary Paget's disease patient-derived xenografts harboring ERBB2 S310F mutation show sensitivity to HER2-targeted therapies." *Oncogene* 39 (36): 5867-5875. https://doi.org/10.1038/s41388-020-01404-x.

Mai, R., S. Zhou, S. Zhou, W. Zhong, L. Hong, Y. Wang, S. Lu, J. Pan, Y. Huang, M. Su, R. Crawford, Y. Zhou, and G. Zhang. 2018. "Transcriptome analyses reveal FOXA1 dysregulation in mammary and extramammary Paget's disease." *Hum Pathol* 77: 152-158. https://doi.org/10.1016/j.humpath.2017.12.030.

Malathi Veeramani, Anand C Damodaran, Sundaram Arunachalam, Tehmin Raj, Subramanian Sundaram, Sandeep Koka Padma. 2022. "Differential Expression of E-cadherin Gene by Real Time RT-PCR and Exon 1 Sequence Analysis in Invasive Breast Carcinoma." *Journal of Clinical and Diagnostic Research* 16 (9): XC01-XC05. https://doi.org/10.7860/jcdr/2022/56502.16872. www.jcdr.net/back_issues.asp?issn=0973-709x&year=2022&month=September&volume=16&issue=9&page=XC01-XC05&id=16872.

Marty, M., F. Cognetti, D. Maraninchi, R. Snyder, L. Mauriac, M. Tubiana-Hulin, S. Chan, D. Grimes, A. Antón, A. Lluch, J. Kennedy, K. O'Byrne, P. Conte, M. Green, C. Ward, K. Mayne, and J. M. Extra. 2005. "Randomized phase II trial of the efficacy and safety of trastuzumab combined with docetaxel in patients with human epidermal growth factor receptor 2-positive metastatic breast cancer administered as first-line treatment: the M77001 study group." *J Clin Oncol* 23 (19): 4265-74. https://doi.org/10.1200/jco.2005.04.173.

Nagata, Y., K. H. Lan, X. Zhou, M. Tan, F. J. Esteva, A. A. Sahin, K. S. Klos, P. Li, B. P. Monia, N. T. Nguyen, G. N. Hortobagyi, M. C. Hung, and D. Yu. 2004. "PTEN activation contributes to tumor inhibition by trastuzumab, and loss of PTEN predicts trastuzumab resistance in patients." *Cancer Cell* 6 (2): 117-27. https://doi.org/10.1016/j.ccr.2004.06.022.

Nahta, R., T. Takahashi, N. T. Ueno, M. C. Hung, and F. J. Esteva. 2004. "P27(kip1) down-regulation is associated with trastuzumab resistance in breast cancer cells." *Cancer Res* 64 (11): 3981-6. https://doi.org/10.1158/0008-5472.Can-03-3900.

Najjar, Mariana K., Sara G. Manore, Angelina T. Regua, and Hui-Wen Lo. 2022. "Antibody-Drug Conjugates for the Treatment of HER2-Positive Breast Cancer." *Genes* 13 (11): 2065. https://www.mdpi.com/2073-4425/13/11/2065.

Nakada, T., T. Masuda, H. Naito, M. Yoshida, S. Ashida, K. Morita, H. Miyazaki, Y. Kasuya, Y. Ogitani, J. Yamaguchi, Y. Abe, and T. Honda. 2016. "Novel antibody drug conjugates containing exatecan derivative-based cytotoxic payloads." *Bioorg Med Chem Lett* 26 (6): 1542-1545. https://doi.org/10.1016/j.bmcl.2016.02.020.

Nonagase, Y., K. Yonesaka, H. Kawakami, S. Watanabe, K. Haratani, T. Takahama, N. Takegawa, H. Ueda, J. Tanizaki, H. Hayashi, T. Yoshida, M. Takeda, Y. Chiba, T. Tamura, K. Nakagawa, and J. Tsurutani. 2016. "Heregulin-expressing HER2-positive breast and gastric cancer exhibited heterogeneous susceptibility to the anti-HER2 agents lapatinib, trastuzumab and T-DM1." *Oncotarget* 7 (51): 84860-84871. https://doi.org/10.18632/oncotarget.12743.

Nordmann, T. M., O. Messerli-Odermatt, L. Meier, S. Micaletto, T. Coppetti, M. Nägeli, J. Kamarachev, K. Kudura, S. N. Freiberger, T. Rordorf, J. Mangana, R. Braun, and R. Dummer. 2019. "Sequential somatic mutations upon secondary anti-HER2 treatment resistance in metastatic ERBB2(S310F) mutated extramammary Paget's disease." *Oncotarget* 10 (62): 6647-6650. https://doi.org/10.18632/oncotarget.27272.

Patnaik, A., L. S. Rosen, S. M. Tolaney, A. W. Tolcher, J. W. Goldman, L. Gandhi, K. P. Papadopoulos, M. Beeram, D. W. Rasco, J. F. Hilton, A. Nasir, R. P. Beckmann, A. E. Schade, A. D. Fulford, T. S. Nguyen, R. Martinez, P. Kulanthaivel, L. Q. Li, M. Frenzel, D. M. Cronier, E. M. Chan, K. T. Flaherty, P. Y. Wen, and G. I. Shapiro. 2016. "Efficacy and Safety of Abemaciclib, an Inhibitor of CDK4 and CDK6, for Patients with Breast Cancer, Non-Small Cell Lung Cancer, and Other Solid Tumors." *Cancer Discov* 6 (7): 740-53. https://doi.org/10.1158/2159-8290.Cd-16-0095.

Pohlmann, P. R., I. A. Mayer, and R. Mernaugh. 2009. "Resistance to Trastuzumab in Breast Cancer." *Clin Cancer Res* 15 (24): 7479-7491. https://doi.org/10.1158/1078-0432.Ccr-09-0636.

Pyla, R. D., R. M. Potekar, V. S. Patil, A. K. Reddy, and K. V. Sathyashree. 2020. "Quantitative mast cell analysis and hormone receptor study (ER, PR and HER2/neu) in invasive carcinoma of breast." *Indian J Pathol Microbiol* 63 (2): 200-204. https://doi.org/10.4103/ijpm.Ijpm_155_19.

Rusnak, D. W., K. Affleck, S. G. Cockerill, C. Stubberfield, R. Harris, M. Page, K. J. Smith, S. B. Guntrip, M. C. Carter, R. J. Shaw, A. Jowett, J. Stables, P. Topley, E. R. Wood, P. S. Brignola, S. H. Kadwell, B. R. Reep, R. J. Mullin, K. J. Alligood, B. R. Keith, R. M. Crosby, D. M. Murray, W. B. Knight, T. M. Gilmer, and K. Lackey. 2001. "The characterization of novel, dual ErbB-2/EGFR, tyrosine kinase inhibitors: potential therapy for cancer." *Cancer Res* 61 (19): 7196-203.

Shen, Y. H., L. Zhang, Y. Gan, X. Wang, J. Wang, S. A. LeMaire, J. S. Coselli, and X. L. Wang. 2006. "Up-regulation of PTEN (phosphatase and tensin homolog deleted on chromosome ten) mediates p38 MAPK stress signal-induced inhibition of insulin signaling. A cross-talk between stress signaling and insulin signaling in resistin-treated human endothelial cells." *J Biol Chem* 281 (12): 7727-36. https://doi.org/10.1074/jbc.M511105200.

Shi, W., T. Jiang, P. Nuciforo, C. Hatzis, E. Holmes, N. Harbeck, C. Sotiriou, L. Peña, S. Loi, D. D. Rosa, S. Chia, A. Wardley, T. Ueno, J. Rossari, H. Eidtmann, A. Armour, M. Piccart-Gebhart, D. L. Rimm, J. Baselga, and L. Pusztai. 2019. "Pathway level alterations rather than mutations in single genes predict response to HER2-targeted therapies in the neo-ALTTO trial." *Ann Oncol* 30 (6): 1018. https://doi.org/10.1093/annonc/mdy530.

Smyth, E. C., M. Nilsson, H. I. Grabsch, N. C. van Grieken, and F. Lordick. 2020. "Gastric cancer." *Lancet* 396 (10251): 635-648. https://doi.org/10.1016/s0140-

6736(20)31288-5.

Sumitomo, C., Y. Iwata, M. Arima, and K. Sugiura. 2023. "A clinicopathological analysis of forkhead box A1 (FOXA1) and estrogen receptor alpha expression in extramammary Paget's disease." *Fujita Med J* 9 (3): 236-239. https://doi.org/10.20407/fmj.2022-030.

Swain, S. M., D. Miles, S. B. Kim, Y. H. Im, S. A. Im, V. Semiglazov, E. Ciruelos, A. Schneeweiss, S. Loi, E. Monturus, E. Clark, A. Knott, E. Restuccia, M. C. Benyunes, and J. Cortés. 2020. "Pertuzumab, trastuzumab, and docetaxel for HER2-positive metastatic breast cancer (CLEOPATRA): end-of-study results from a double-blind, randomised, placebo-controlled, phase 3 study." *Lancet Oncol* 21 (4): 519-530. https://doi.org/10.1016/s1470-2045(19)30863-0.

Swain, S. M., M. Shastry, and E. Hamilton. 2023. "Targeting HER2-positive breast cancer: advances and future directions." *Nat Rev Drug Discov* 22 (2): 101-126. https://doi.org/10.1038/s41573-022-00579-0.

Takeichi, T., Y. Okuno, T. Matsumoto, N. Tsunoda, K. Suzuki, K. Tanahashi, M. Kono, T. Kikumori, Y. Muro, and M. Akiyama. 2020. "Frequent FOXA1-Activating Mutations in Extramammary Paget's Disease." *Cancers (Basel)* 12 (4). https://doi.org/10.3390/cancers12040820. https://mdpi-res.com/d_attachment/cancers/cancers-12-00820/article_deploy/cancers-12-00820.pdf?version=1585473837.

Tanaka, R., Y. Sasajima, H. Tsuda, K. Namikawa, A. Takahashi, A. Tsutsumida, Y. Fujisawa, M. Fujimoto, and N. Yamazaki. 2016. "Concordance of the HER2 protein and gene status between primary and corresponding lymph node metastatic sites of extramammary Paget disease." *Clin Exp Metastasis* 33 (7): 687-97. https://doi.org/10.1007/s10585-016-9804-z.

Tanaka, R., Y. Sasajima, H. Tsuda, K. Namikawa, A. Tsutsumida, F. Otsuka, and N. Yamazaki. 2013. "Human epidermal growth factor receptor 2 protein overexpression and gene amplification in extramammary Paget disease." *Br J Dermatol* 168 (6): 1259-66. https://doi.org/10.1111/bjd.12249.

Thomas, A., B. A. Teicher, and R. Hassan. 2016. "Antibody-drug conjugates for cancer therapy." *Lancet Oncol* 17 (6): e254-e262. https://doi.org/10.1016/s1470-2045(16)30030-4.

Tokuchi, K., T. Maeda, S. Kitamura, T. Yanagi, and H. Ujiie. 2022. "HER2-Targeted Antibody-Drug Conjugates Display Potent Antitumor Activities in Preclinical Extramammary Paget's Disease Models: In Vivo and Immunohistochemical Analyses." *Cancers (Basel)* 14 (14). https://doi.org/10.3390/cancers14143519.

von Minckwitz, G., M. Procter, E. de Azambuja, D. Zardavas, M. Benyunes, G. Viale, T. Suter, A. Arahmani, N. Rouchet, E. Clark, A. Knott, I. Lang, C. Levy, D. A. Yardley, J. Bines, R. D. Gelber, M. Piccart, and J. Baselga. 2017. "Adjuvant Pertuzumab and Trastuzumab in Early HER2-Positive Breast Cancer." *N Engl J Med* 377 (2): 122-131. https://doi.org/10.1056/NEJMoa1703643.

Vornicova, O., D. Hershkovitz, T. Yablonski-Peretz, O. Ben-Itzhak, Z. Keidar, and G. Bar-Sela. 2014. "Treatment of metastatic extramammary Paget's disease associated with adnexal adenocarcinoma, with anti-HER2 drugs based on genomic alteration ERBB2 S310F." *Oncologist* 19 (9): 1006-7. https://doi.org/10.1634/theoncologist.2014-0054.

Wang, Y., Y. Liu, Y. Du, W. Yin, and J. Lu. 2013. "The predictive role of phosphatase and tensin homolog (PTEN) loss, phosphoinositol-3 (PI3) kinase (PIK3CA) mutation, and PI3K pathway activation in sensitivity to trastuzumab in HER2-positive breast cancer: a meta-analysis." *Curr Med Res Opin* 29 (6): 633-42. https://doi.org/10.1185/03007995.2013.794775.

Wang, Z. H., Z. Q. Zheng, S. C. Jia, S. N. Liu, X. F. Xiao, G. Y. Chen, W. Q. Liang, and X. F. Lu. 2022. "Trastuzumab resistance in HER2-positive breast cancer: Mechanisms, emerging biomarkers and targeting agents." *Front Oncol* 12: 1006429. https://doi.org/10.3389/fonc.2022.1006429.

Wu, X., H. Yang, X. Yu, and J. J. Qin. 2022. "Drug-resistant HER2-positive breast cancer: Molecular mechanisms and overcoming strategies." *Front Pharmacol* 13: 1012552. https://doi.org/10.3389/fphar.2022.1012552.

Yanagi, T., M. Krajewska, S. Matsuzawa, and J. C. Reed. 2014. "PCTAIRE1 phosphorylates p27 and regulates mitosis in cancer cells." *Cancer Res* 74 (20): 5795-807. https://doi.org/10.1158/0008-5472.Can-14-0872.

Yoshino, K., Y. Fujisawa, Y. Kiyohara, T. Kadono, Y. Murata, H. Uhara, N. Hatta, H. Uchi, S. Matsushita, T. Takenouchi, T. Hayashi, and K. Ohara. 2016. "Usefulness of docetaxel as first-line chemotherapy for metastatic extramammary Paget's disease." *J Dermatol* 43 (6): 633-7. https://doi.org/10.1111/1346-8138.13200.

Yue, C., Y. Bai, Y. Piao, and H. Liu. 2021. "DOK7 Inhibits Cell Proliferation, Migration, and Invasion of Breast Cancer via the PI3K/PTEN/AKT Pathway." *J Oncol* 2021: 4035257. https://doi.org/10.1155/2021/4035257.

Zhang, G., S. Zhou, W. Zhong, L. Hong, Y. Wang, S. Lu, J. Pan, Y. Huang, M. Su, R. Crawford, Y. Zhou, and R. Mai. 2019. "Whole-Exome Sequencing Reveals Frequent Mutations in Chromatin Remodeling Genes in Mammary and

Extramammary Paget's Diseases." *J Invest Dermatol* 139 (4): 789-795. https://doi.org/10.1016/j.jid.2018.08.030.

Zhu, H., and D. J. Lewis. 2022. "Efficacy of trastuzumab in HER-2-positive advanced extramammary Paget's disease." *Expert Opin Biol Ther* 22 (5): 673-674. https://doi.org/10.1080/14712598.2022.2066472.